doi:10.1093/plphys/kiaa029 PLANT PHYSIOLOGY 2021: 185: 295–317

Plant Physiology

Research Article

Sugar modulation of anaerobic-response networks in maize root tips

Maria-Angelica Sanclemente ,[1,2,3,*,†] Fangfang Ma,[1,2,4] Peng Liu ,[1,2,5] Adriana Della Porta ,[1] Jugpreet Singh ,[1,2] Shan Wu ,[1] Thomas Colquhoun ,[1,6] Timothy Johnson ,[1,6] Jiahn-Chou Guan,[2] and Karen E. Koch [1,2]

1 Plant Molecular and Cellular Biology, University of Florida, Gainesville, Florida 32611, USA
2 Horticultural Sciences, University of Florida, Gainesville, Florida 32611, USA
3 Plant Ecophysiology, Institute of Environmental Biology, Utrecht University, Utrecht 3584CH, The Netherlands
4 Horticultural Sciences, Shandong Agricultural University, Taian, Shandong, China
5 Donald Danforth Plant Science Center, St. Louis, Missouri 63132, USA
6 Environmental Horticulture, University of Florida, Gainesville, Florida, USA

*Author for communication: sanangelma@gmail.com
†Senior author.

M.A.S. and K.E.K. conceived, designed, and supervised the project; M.A.S. and A.D.P. performed the experiments; S.W. constructed RNA-seq libraries; M.A.S. extracted metabolites for quantification; F.M. analyzed metabolite quantification by GC-MS and LC-MS-MS; T.J. and T.C. provided technical assistance to F.M.; M.A.S., P.L. and J.S. analyzed transcriptome data; M.A.S. conducted statistical analyses; J.C.G. analyzed qPCR; M.A.S. and K.E.K. interpreted results and wrote the manuscript with contributions from all the authors. M.A.S. agrees to serve as the author responsible for contact and ensures communication.

The author responsible for distribution of materials integral to the findings presented in this article in accordance with the policy described in the Instructions for Authors (https://academic.oup.com/plphys) is: Maria-Angelica Sanclemente (sanangelma@gmail.com).

Abstract

Sugar supply is a key component of hypoxia tolerance and acclimation in plants. However, a striking gap remains in our understanding of mechanisms governing sugar impacts on low-oxygen responses. Here, we used a maize (*Zea mays*) root-tip system for precise control of sugar and oxygen levels. We compared responses to oxygen (21 and 0.2%) in the presence of abundant versus limited glucose supplies (2.0 and 0.2%). Low-oxygen reconfigured the transcriptome with glucose deprivation enhancing the speed and magnitude of gene induction for core anaerobic proteins (ANPs). Sugar supply also altered profiles of hypoxia-responsive genes carrying G4 motifs (sources of regulatory quadruplex structures), revealing a fast, sugar-independent class followed more slowly by feast-or-famine-regulated G4 genes. Metabolite analysis showed that endogenous sugar levels were maintained by exogenous glucose under aerobic conditions and demonstrated a prominent capacity for sucrose re-synthesis that was undetectable under hypoxia. Glucose abundance had distinctive impacts on co-expression networks associated with ANPs, altering network partners and aiding persistence of interacting networks under prolonged hypoxia. Among the ANP networks, two highly interconnected clusters of genes formed around *Pyruvate decarboxylase 3* and *Glyceraldehyde-3-phosphate dehydrogenase 4*. Genes in these clusters shared a small set of *cis*-regulatory elements, two of which typified glucose induction. Collective results demonstrate specific, previously unrecognized roles of sugars in low-oxygen responses, extending from accelerated onset of initial adaptive phases by starvation stress to maintenance and modulation of co-expression relationships by carbohydrate availability.

Received July 7, 2020. Accepted October 28, 2020. Advance access publication December 25, 2020

Introduction

The role of oxygen extends beyond its essentiality as a substrate for oxidative phosphorylation during ATP production in mitochondria. Many sensing, metabolic, and synthetic processes require oxygen either as a substrate or as a signaling molecule (Bailey-Serres and Voesenek, 2008; van Dongen and Licausi, 2015). Diverse effects of oxygen deficiency (hypoxia) can thus occur whenever levels drop below the physiological threshold needed to sustain normal metabolism and signaling. Among these, the best-known change occurs in ATP production, which quickly shifts from an aerobic yield of 36 ATP per glucose to only 2 ATP from glycolysis and fermentation (Bailey-Serres and Voesenek, 2008; van Dongen and Licausi, 2015).

Other impacts of hypoxia are evident in a rapid reconfiguration of the transcriptome, a process strongly responsive to the fast, oxygen-dependent changes in longevity for group VII ethylene response factors (VII-ERFs). These VII-ERF proteins turn over rapidly when oxygen is present, since their degradation is mediated by the N-end rule (Gibbs et al., 2011; Licausi et al., 2011). In Arabidopsis (*Arabidopsis thaliana*), hypoxic stabilization of the VII-ERF protein-related to APETALA 2.12 initiates anaerobic responses at the level of gene expression within 30 min (Gibbs et al., 2011; Licausi et al., 2011). However, targeted modification of breakdown regulated by the N-end rule leads to transcriptome profiles that only partially mimic those associated with low oxygen (Gibbs et al., 2011), thus indicating additional factors are involved in oxygen responses.

Additional signals that contribute to hypoxia acclimation may also arise from the rapid adjustment of cellular metabolism essential for sustaining energy balance and redox status when oxygen is limiting. This possibility is consistent with observed contributions by plant energy sensors, such as the sucrose nonfermenting1-related kinase1 (SnRK1) and target of rapamacyn (TOR), to starvation signals during hypoxia (Baena-González et al., 2007; Tomé et al., 2014; Cho et al., 2019; Ramon et al., 2019).

Starvation is often a central feature of hypoxic metabolism, so it is not surprising that sugar-sensing systems have been implicated in the acclimation process (Cho et al., 2021). Prominent examples include the sugar modulation of at least two genes for core anaerobic proteins (ANPs) in grains and Arabidopsis. The *Alcohol dehydrogenase1* (*Adh1*) gene for alcohol dehydrogenase is sugar-responsive, and so too is the maize *Sh1* gene for sucrose synthase (Koch et al., 1992, 2000; Lee et al., 2009; Loreti et al., 2018). A second maize sucrose synthase (*Sus1*) also responds to both sugars and low oxygen (Koch et al., 1992). Furthermore, two sucrose synthase genes (SUS1 and SUS4) in Arabidopsis are also sugar-modulated (Loreti et al., 2005; Bieniawska et al., 2007; Santaniello et al., 2014). Some of these genes are induced by sugar abundance, others by starvation, which together provide a means of adjusting low-oxygen responses to changing substrate availabilities. Since sucrose synthases typically cleave sucrose in vivo, their upregulation under hypoxia can enhance the potential for sucrose partitioning to an ATP-conserving path of glycolysis, as well as minimizing flux through the hexokinase (HXK)-based sugar-sensing system, and sustaining fermentation pathways (Zeng et al., 1998,, 1999; Koch, 2004; van Dongen and Licausi, 2015).

Impacts of sugar-sensing systems on transcription and translation are distinct from direct effects of substrate limitation on metabolism, but both would be involved in low-oxygen responses. Fine-tuned signals of sugar availability arise from "moonlighting" metabolic enzymes with dual roles in signal transduction (e.g., HXK), and also from systems that sense oxidant–antioxidant balance (e.g., superoxide dismutase; Koch, 1996; Couée et al., 2006; Rolland et al., 2006; Baena-González et al., 2007; Keunen et al., 2013; Tomé et al., 2014). In contrast, direct metabolic effects would include those of ATP availability and feedback mechanisms. Together, both systems couple sugar and oxygen status with activity at cellular and organellar levels that mediate carbon metabolism, redox homeostasis, and energy production. In photosynthetic source tissues, for example, injury by hypoxia is minimized by photosynthetic production of sugars as well as oxygen in the chloroplast (Couée et al., 2006; Shingaki-Wells et al., 2014). However, in sucrose-importing sink tissues, mitochondrial integrity and redox status are tightly regulated by endogenous and exogenous sugar levels (Vartapetian and Andreeva, 1986; Couée et al., 2006; Kim et al., 2006; Shingaki-Wells et al., 2014). Effects of sugar sensing are also important in the modulation of translation efficiency through ribosome biogenesis and polysome occupancy (Rahmani et al., 2009; Gamm et al., 2014; Morgan et al., 2019; Parenteau et al., 2019). Collective costs of transcription, translation, and protein turnover confer an energetic advantage to the rapid repression observed for most mRNAs when oxygen is limiting (Branco-Price et al., 2008). Only a few genes are successfully expressed, such as the abundant ANPs characteristic of hypoxic responses (Sachs et al., 1980; Mustroph et al., 2009). Carbohydrate metabolism is thus central to low-oxygen responses as a source of both direct and indirect effectors. The extent of these inputs and their underlying mechanisms remains unclear despite their ultimate importance to acclimation and survival.

A newly described component of sugar- and oxygen-regulated gene expression in eukaryotes comes from guanine (G)-rich sequences of nucleic acids that can form four-stranded, secondary structures known as G4-quadruplexes (G4s; Kendrick and Hurley 2010; Clark et al., 2012; Fleming et al., 2015, 2017). In maize, G4 sequences are prevalent in 5′-UTRs (Un-Translated Regions) of genes for sugar metabolism, energy sensing, and low-oxygen responses, including *Sh1*, *Snrk1*, and several hypoxia-induced transcription factors among the group VII-ERFs (Andorf et al., 2014). Due to their high G-content, G4s are highly sensitive to oxidative damage (Clark et al., 2012). Oxidation of G4-DNA during hypoxia produces 8-oxo-7,8-dihydroguanine (OG), which acts as an epigenetic mark leading to enhanced expression of downstream genes (Fedeles, 2017; Fleming et al., 2017). These OG

marks have been identified in G4-sequences located in the promoters of many hypoxia-regulated genes, including the mammalian oxygen sensor hypoxia-inducible factor 1-alpha (Fleming et al., 2015, 2017). Suggested contributions by G4s to regulation of gene expression thus extend to low oxygen and sugar responses. However, the potential roles of G4s in plants remain largely unexplored.

The interface between sugar and oxygen responses has been difficult to dissect. Initial work identified the first set of core mRNAs for ANPs in plants and the direct role of sugars in their regulation (Sachs et al., 1980, 1996; Koch et al., 1992; Zeng et al., 1998,, 1999). The maize root-tip system was central to these efforts, and interactions were further explored in early micro-array studies by Loreti et al. (2005) in Arabidopsis seedlings and by Lasanthi-Kudahettige et al. (2009) in rice (*Oryza sativa*) coleoptiles. Subsequent research, however, focused on separate effects of hypoxia and sugar availability at different levels of regulation. Our goal was thus to distinguish which components of the hypoxic response are sugar-responsive and which might be independent of carbohydrate status. To do so, we modified a flow-through culture system for excised maize root-tips (Saglio et al., 1980; Koch et al., 1992), which allows a precise control of both sugar and oxygen availability. Use of glucose as the sole sugar substrate provided a direct path of entry into central metabolism that bypassed the variability otherwise observed with partial action of cell-wall invertases on exogenously supplied sucrose.

Here, we separated sugar-modulated components of transcriptome responses to low-oxygen and identified differential contributions by genes favored under feast and famine conditions. Starvation had a positive initial effect on mRNAs for ANPs, consistent with a stress contribution to their hypoxic induction. However, glucose abundance was central to sustaining co-expression relationships within and between ANP-associated networks over time. Glucose availability also favored upregulation of hypoxia-responsive genes having G4 motifs. In addition, we showed that *Pyruvate decarboxylase* (*Pdc3*) and *glyceraldehyde-3-phosphate dehydrogenase* (*Gpc4*) were highly interconnected at the co-expression level and that their partners in these networks were determined by glucose availability. Further investigation of underlying mechanisms revealed that genes in the *Gpc4-Pdc3* modules were co-regulated by a small set of *cis*-elements, two of which were distinct to genes expressed when glucose was abundant. Work here provides new evidence for distinct contributions by sugar availability as a central component of the signals for transcriptional regulation during hypoxia.

Results

Fewer genes were impacted by sugars than oxygen, but starvation responses increased during hypoxia

To identify transcriptional and metabolic modifications initiated by altered availability of oxygen and sugars, we exposed 6-mm root tips from 3-d-old maize seedlings to 24 h of two different oxygen levels (ambient air at 21% v/v or low oxygen at 0.2% v/v) in combination with two glucose concentrations [physiologically abundant at 2% w/v {111 mM} or low at 0.2% w/v {11.1 mM}]. These glucose treatments were selected based on responses of maize root tips under low-oxygen (Saglio et al., 1980; Bouny and Saglio, 1996), as well as basal levels of endogenous glucose in intact roots (~80 mM; Saglio et al., 1980; Saglio and Pradet, 1980; Brouquisse et al., 1991; Dieuaide-Noubhani et al., 1995), and previous work with this system (Brouquisse et al., 1991; Koch et al., 1992; Bouny and Saglio, 1996; Alonso et al., 2007). The minimal-glucose treatment (0.2% w/v) maintains root-tip responsiveness and sucrose synthase activity for at least 48 h under aerobic conditions (Koch et al., 1992). Conversely, the physiologically abundant glucose (AG) supports maximal growth rate and respiratory capacity (Saglio and Pradet 1980; Koch et al., 1992; Bouny and Saglio 1996). To test the efficacy of the current system, we quantified the accumulation of two low-oxygen markers: *Adh1* and *Adh2* transcripts. As expected, their abundance rose markedly and was sustained throughout the 24-h period (Supplemental Figure S1A).

To characterize concurrent alterations in root-tip growth and transcriptome profiles under the conditions tested, rates of tip extension were monitored throughout these studies. Oxygen impacted the elongation more prominently than did sugar availability (Supplemental Figure S1B). When oxygen and glucose (2.0%) were both abundant, root-tip growth rates were about 25% greater than when sugar supplies were limited. This difference was evident only under the aerobic conditions necessary for long-term elongation (Koch et al., 1992). In contrast, hypoxic root tips ceased growth after only 3 h. Prior to this point, initial elongation rates were equivalent to those of aerobic controls with abundant exogenous glucose.

These changes were compared to coincident restructuring of the root transcriptome analyzed by RNA-seq during the same time-course. Hierarchical gene clustering showed that genome-wide effects of hypoxia were evident within 3 h (Figure 1A). Differential responses to sugar and oxygen availability were also indicated over time by principal component analysis, which separated oxygen effects on the *x*-axis (Supplemental Figure S2A), and glucose treatments over time on the *y*-axis (Supplemental Figure S2, B and C) when aerobic and hypoxic conditions were shown separately. Duration was a prominent effector, evident in the transcriptomes from hypoxic treatments with low versus AG initially clustering together at 3 and 6 h. The initial responses also indicated that effects of oxygen were considerably greater than those of carbohydrates during onset of hypoxia.

To contrast the magnitude of transcriptional restructuring in terms of gene numbers affected, we separated sugar and oxygen effects over time. We first focused on the sugar-responsive genes [mRNAs for differentially expressed genes {DEGs}] by comparing transcriptomes from low-glucose to abundant-glucose treatments under either ambient air or low oxygen (Figure 1B; Supplemental Dataset S1). Conversely, we followed transcriptomes from low-oxygen and ambient-air treatments in the presence of either low or AG (Figure 1C; Supplemental Dataset S2). Overall, we

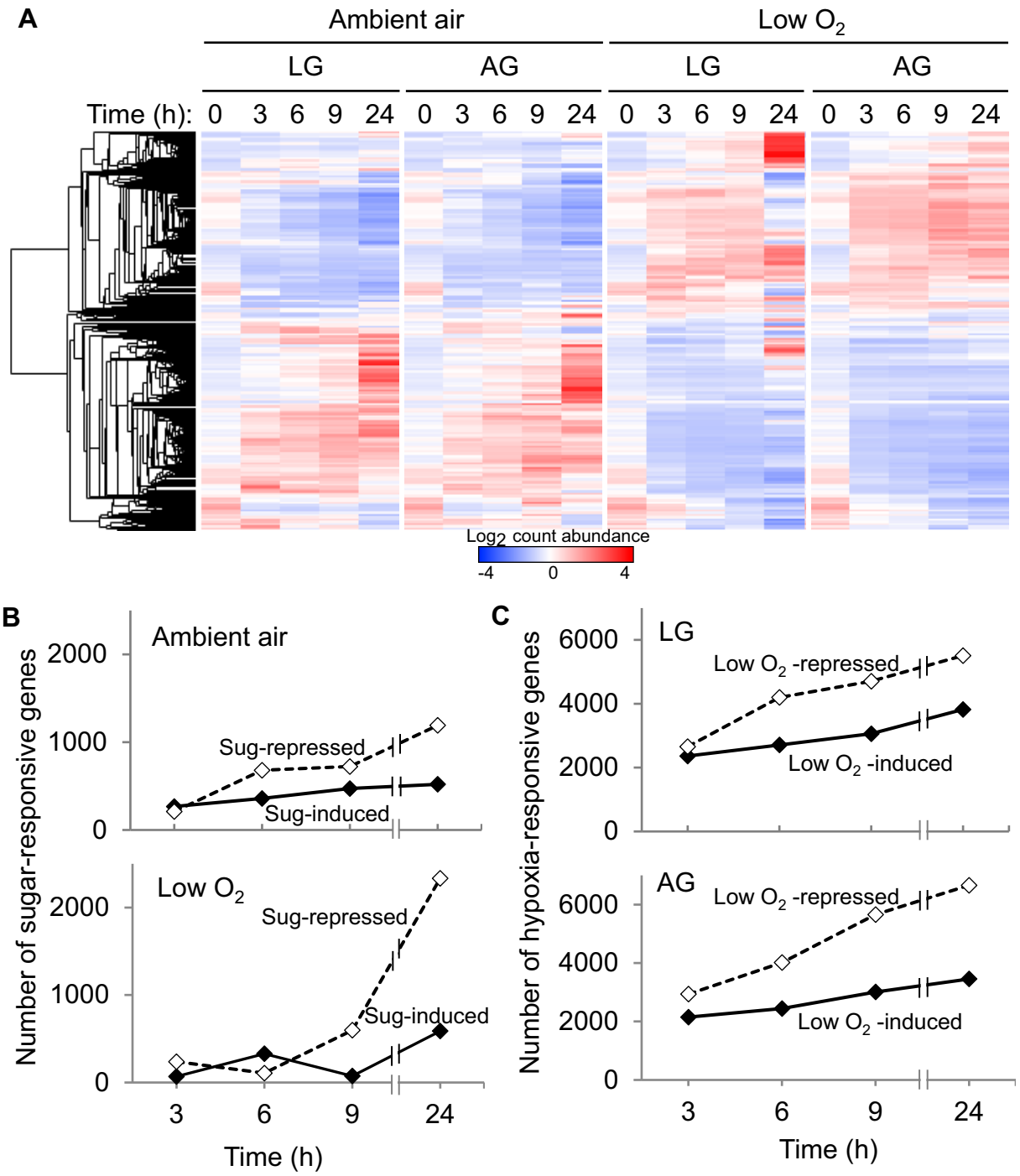

Figure 1 Root transcriptome responses to different levels of oxygen and sugar. (**A**) Hierarchical clustering analysis of normalized samples using average linkage based on Euclidean distance revealed significant differences (two-fold change, $P < 0.05$) between oxygen and sugar levels. (**B**) Number of sugar-responsive genes that were differentially expressed ($P < 0.05$) in ambient air and low oxygen (low O_2). (**C**) Number of hypoxia-responsive genes differentially expressed at each glucose level (LG or AG). Treatments included two oxygen levels: ambient air (21% O_2 v/v) or low oxygen (0.2% O_2 v/v) in combination with two glucose concentrations: LG (0.2% w/v) or AG (2% w/v).

observed, first, that the maximal number of sugar-responsive genes under low oxygen was less than half that affected by hypoxia (compare the *y*-axis of Figure 1, B and C), and second, that low oxygen increased the number of starvation-induced (sugar-repressed) genes to an increasing degree over time (Figure 1B).

Glucose altered transcriptome composition under low oxygen

Functional classes of transcripts were identified among the sugar- and oxygen-responsive genes using the Pageman tool (Usadel et al., 2006). Regardless of glucose levels, hypoxia upregulated genes categorized by gene ontology (GO) terms

for carbohydrate metabolism, glycolysis, and response to stress (Figure 2A). In contrast, transcripts for energy-expensive processes, such as biosynthesis of cell wall and secondary metabolites, were downregulated. Interestingly, we observed a significant representation of transcripts for sucrose synthesis, indicating that mRNAs for this energetically expensive process persist even under low-oxygen conditions (Figure 2A).

The GO categories enriched among oxygen-responsive genes (Figure 2A) typically included those found to be sugar-responsive (Figure 2B). However, transcripts for ribosomal proteins were distinctively represented only when glucose was abundant (Figure 2, A and B). This significant enrichment of ribosomal transcripts was independent of oxygen levels, indicating that sugar positively altered their accumulation. In contrast, abundance of typically sugar-repressed mRNAs for photosynthetic-related genes was elevated by hypoxia, regardless of sugar levels. Such responses are not uncommon, even in normally nonphotosynthetic tissues (Dinneny et al., 2008; Sasidharan et al., 2013; van Veen et al., 2016). In the present work, mRNAs for light-harvesting complexes were over-represented in root tips from both oxygen treatments (Figure 2, A and B). Similar results have been reported for roots of submerged Arabidopsis and *Rorippa* species (Sasidharan et al., 2013; van Veen et al., 2016). Underlying mechanisms remain unknown but could include stress-related changes in energy charge and/or carbohydrate availability. Although traces of light can induce some degree of plastid development in roots (Armstrong and Armstrong, 1994; Dinneny et al., 2008), the hypoxic upregulation of photosynthetic genes in Arabidopsis roots seems to be light-independent (Sasidharan et al., 2013; van Veen et al., 2016). Moreover, this induction of photosynthetic genes in roots can occur in response to salt stress, reactive oxygen species (ROS) accumulation, and Pi starvation (Dinneny et al., 2008; Kang et al., 2014). The biological significance of these responses is yet to be determined, but data here and elsewhere indicate a conservation between monocots and dicots.

Sugar depletion enhanced accumulation of mRNAs for core anaerobic genes of maize

To evaluate the extent of sugar effects on low-oxygen responses, we identified mRNAs that varied most prominently during progression of transcriptome changes (Figure 3). The 10 most strongly induced transcripts encoded primarily mRNAs for ANPs that contribute to the core hypoxia response of maize (Sachs et al., 1980). These proteins are selectively translated during hypoxia and participate in carbohydrate metabolism, glycolysis, and fermentation (Sachs et al., 1980; Mustroph et al., 2009). Enhancement of mRNA levels for these core-hypoxia genes was greater when glucose was limiting. Starvation thus positively modulated accumulation of these key transcripts. The converse was also evident in the attenuation of this response by AG.

Given the magnitude of starvation enhancement observed here for hypoxic induction of the ANP mRNAs (Figure 3), we sought to determine how widespread this response was among genes for primary metabolism (Figure 4). The mRNAs for *Sus1* and *Sh1*, the two main sucrose synthases that reversibly cleave sucrose *in vivo*, were prominent in maize roots, and levels of both increased under hypoxia (Figure 4, A and B). Abundance of *Sus1* transcripts was unaffected by glucose availability in these analyses. In contrast, the extent of induction for *Sh1* mRNA under low oxygen was enhanced when glucose was limited. This response of *Sh1* was similar to that observed for other ANPs, with key genes among them validated by reverse transcription quantitative PCR (RT-qPCR) analysis at specific time points (Supplemental Figure S3). In Arabidopsis, limitations to sugar supply are also implicated in the extent of induction and apparent roles of sucrose synthases under low-oxygen (Santaniello et al., 2014). Here, the alternate, unidirectional path of sucrose cleavage was represented by *Invertase* transcripts that were much less abundant, and except for *cell-wall invertase* (*Cw1*), levels of all other *Invertase* mRNAs were further reduced by hypoxia (Figure 4B). Data are consistent with a predominant capacity for sucrose cleavage by the sucrose synthase pathway in maize root tips, particularly under hypoxia (Ricard et al., 1998; Koch, 2004; Bieniawska et al., 2007; Wang et al., 2014).

Low-oxygen tolerance in maize has been associated with the capacity to maintain HXK activity (Bouny and Saglio, 1996; Gharbi et al., 2007). There are nine *Hxk* genes in maize. Of these, only mRNAs for the *Hxk7* (Zm00001d037689) accumulated under hypoxia in the current work (Figure 4B). Initial responses of this transcript to limiting oxygen supplies were evident within 3 h and continued for 24 h. As observed for the ANPs, abundance of the *Hxk7* mRNAs was maximized by progressive glucose depletion under hypoxia. Transcripts associated with fermentative pathways, including *Adh1*, *Adh2*, and several *Pdcs*, were highly induced by hypoxia while levels of *Lactate dehydrogenase* (*Ldh*) remained constant throughout all treatments. Nevertheless, high levels of *Adh* and *Pdc* mRNAs were observed at the experiment start (0 h) as well as under aerobic conditions, consistent with at least partial functioning of hypoxic metabolism in normal young roots (Sachs et al., 1980; Thomson and Greenway, 1991; Drew, 1997). In addition, the modest accumulation of *Adh1* transcripts under aerobic conditions was greater when glucose was abundant, indicating that sugar effects can differ with oxygen environment. Previous work shows that Arabidopsis seedlings are unable to maintain *Adh* induction during anoxia unless exogenous sucrose is provided (Loreti et al., 2005) or starch reserves are present (Loreti et al., 2018). Here, in hypoxic maize root tips, even minimal amounts of glucose (0.2%) were sufficient to prolong duration of elevated transcript abundance for *Adh*.

Levels of mRNAs related to biosynthesis of sucrose were prominent in root tips, regardless of whether these tips were intact, excised, or incubated with differing levels of glucose (Figure 4, C and D). Still further enhancement occurred

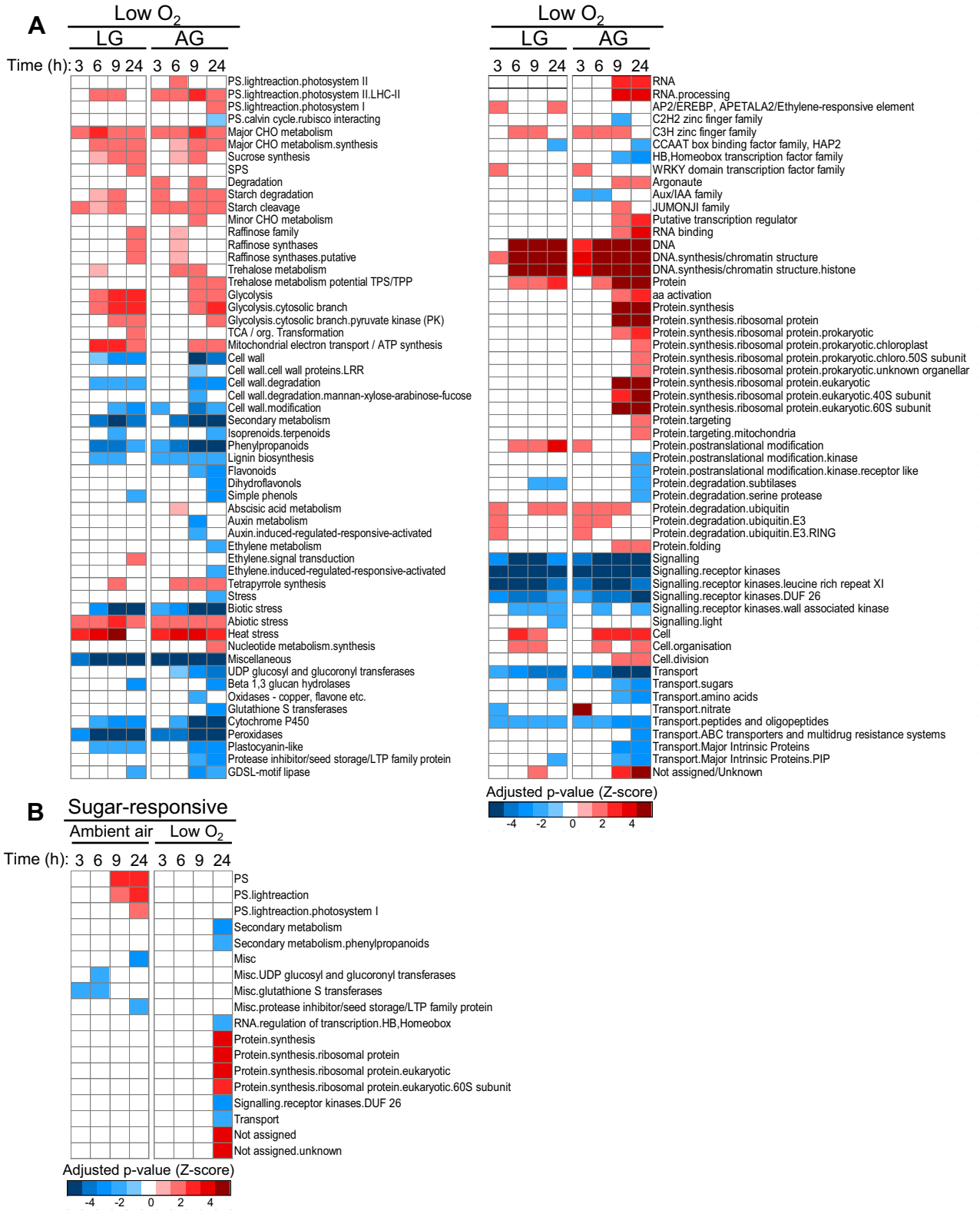

Figure 2 GO-term enrichment among sugar- and oxygen-responsive genes over time. (**A**) functional categories of transcripts over- (red) or under-represented (blue) in root-tips exposed to low oxygen (Low O_2; 0.2% v/v) with either LG (0.2% w/v) or AG (2% w/v). (**B**) GO categories over- (red) or under-represented (blue) among glucose-responsive genes under ambient air (21% O_2 v/v) or low oxygen (Low O_2; 0.2% O_2 v/v). Data were analyzed using the Wilcoxon test in Pageman ($P < 0.05$, Usadel et al., 2006) and resulting heat-maps indicate log2 changes during treatments.

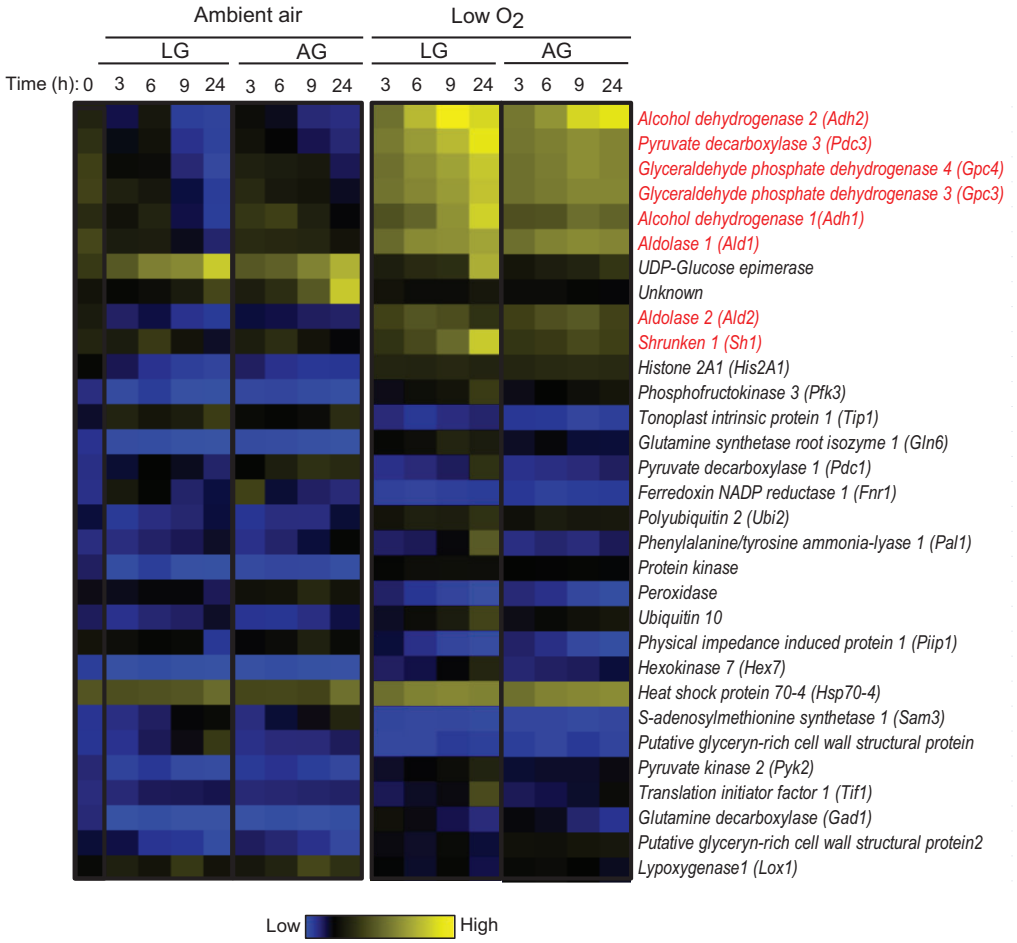

Figure 3 Changes in relative gene expression during responses to oxygen and sugar treatments over time. The heatmap represents the top 30 genes with the greatest statistical variance and shows treatment effects on expression of each gene relative to its overall standard deviation. Treatments included two levels of glucose: LG (0.2% w/v) or AG (2% w/v) in combination with two oxygen treatments: ambient air (21% O_2 v/v) and low oxygen (Low O_2; 0.2% v/v). Red text indicates genes that encode the core "ANPs" initially identified using maize by Sachs et al. (1980). Transcripts are ranked based on significant differences in their relative expression ($P < 0.05$; Supplemental Datasets S1 and S2).

in response to hypoxia. *Sucrose phosphate synthase* (*Sps*) and *sucrose phosphate phosphatase* (*Spp*) were both induced under low oxygen regardless of sugar levels. These results indicate that limited substrate supplies for primary metabolism may induce genes for enzymes of sucrose biosynthesis, possibly advantageous under short-term hypoxia, even when this may be an energy-expensive process.

Results observed here indicate that glucose levels can modulate the hypoxia response in maize roots. Although glucose deprivation enhances the low-oxygen induction of core hypoxic genes and transcripts related to anaerobic metabolism, AG supplies attenuate these responses. Representation of these genes in the anaerobic transcriptome is thus responsive to sugar status.

Rapid hypoxic induction of G4 genes is initially sugar-independent, later feast-or-famine modulated

Over a quarter of maize genes (9,572; 28%) carry sequences for G4 quadruplex formation (Andorf et al., 2014). These four-stranded, localized configurations occur most often near transcription start sites from which they can regulate gene expression (Postel et al., 1993; Clark et al., 2012; Welsh et al., 2013; Andorf et al., 2014; Fedeles, 2017; Fleming et al., 2017). In maize, G4s are prevalent in many genes that respond to low energy and low oxygen (Andorf et al., 2014). Previously, we and others proposed that one role of G4s could be that of pausing transcription of key genes that could later be mobilized rapidly in response to signals of severe stress. We thus hypothesized that here, mRNAs from G4-containing genes would be disproportionately abundant among the earliest responders. To test this possibility and explore dynamics of G4-containing genes during low oxygen, we compared the entirety of our hypoxia-regulated mRNAs (in low or AG) to those identified in a whole-genome screen for G4 sequences in maize by Andorf et al. (2014).

Figure 5A shows that hypoxia did indeed upregulate a significantly greater percentage of G4 genes than are present in the genome or expressed in untreated maize root tips.

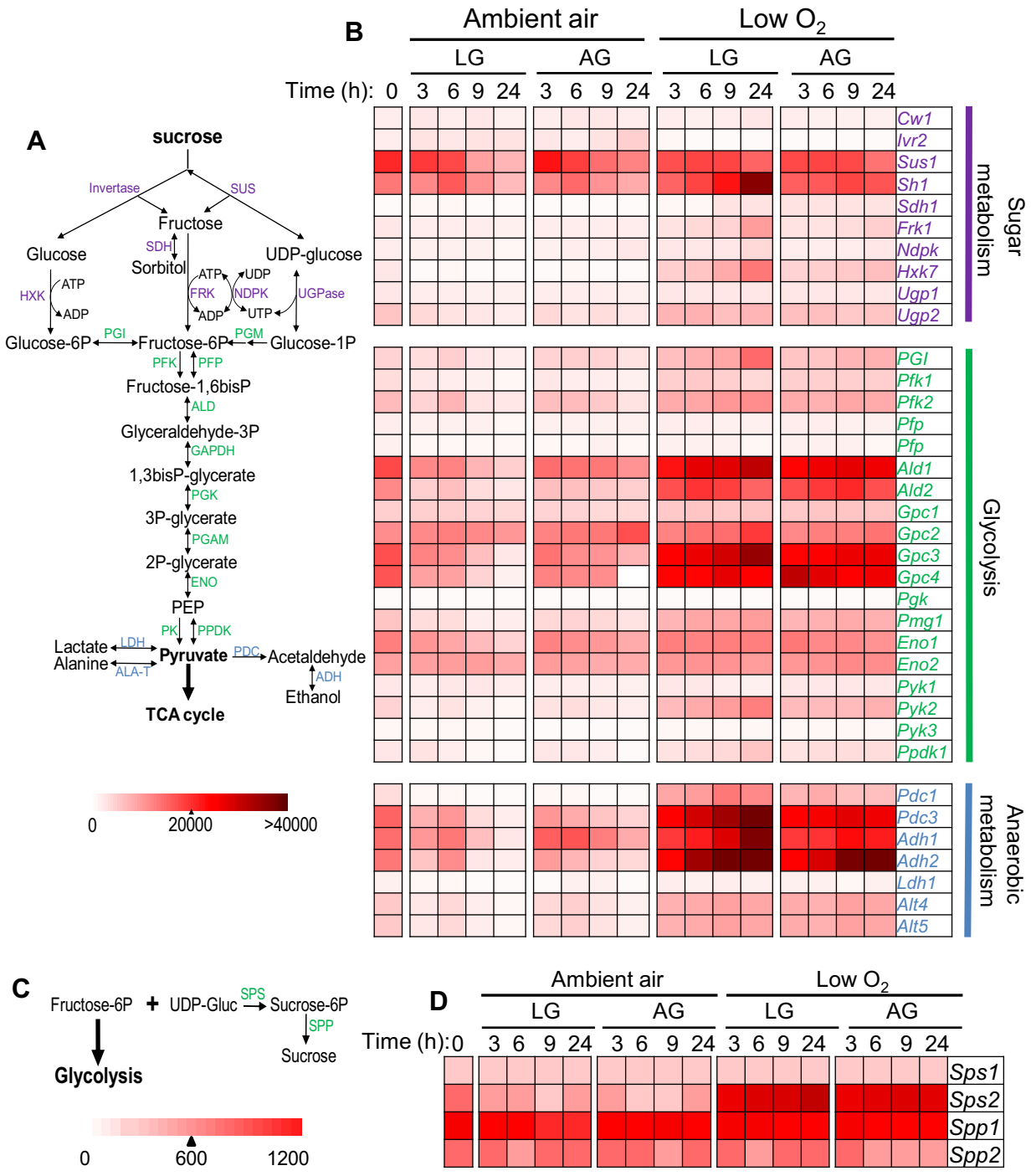

Figure 4 Effect of glucose levels on transcript profiles associated with primary and anaerobic metabolism over time. (**A**) Schematic representation of reactions associated with primary and hypoxic metabolism. (**B**) Heat-map of mRNA abundance (rlog-transformed, normalized count values) for transcripts associated with pathways in A. (**C**) Schematic representation of SPS and SPP reactions. (**D**) Heat-map of relative RNA abundance as number of normalized sequence reads (rlog-transformed) genes encoding SPS and SPP. Treatments included two levels of glucose: LG (0.2% w/v) or AG (2% w/v) in combination with two oxygen treatments: ambient air (21% O_2 v/v) and low oxygen (Low O_2; 0.2% v/v). Significance of sugar effects on gene expression was evaluated at each time point using the DESEq2 pipeline (Supplemental Dataset S1).

Moreover, the response was rapid, with maximum numbers of G4 genes induced in less than 3 h. Interestingly, the proportion of genes that contain G4s remained constant throughout the treatments and was similar in both glucose levels (Figure 5, A and B; Supplemental Dataset S3). However, the identities of these genes changed over time, with rapid, initial regulation being sugar-independent, and later mRNAs separating into feast-or-famine modulated

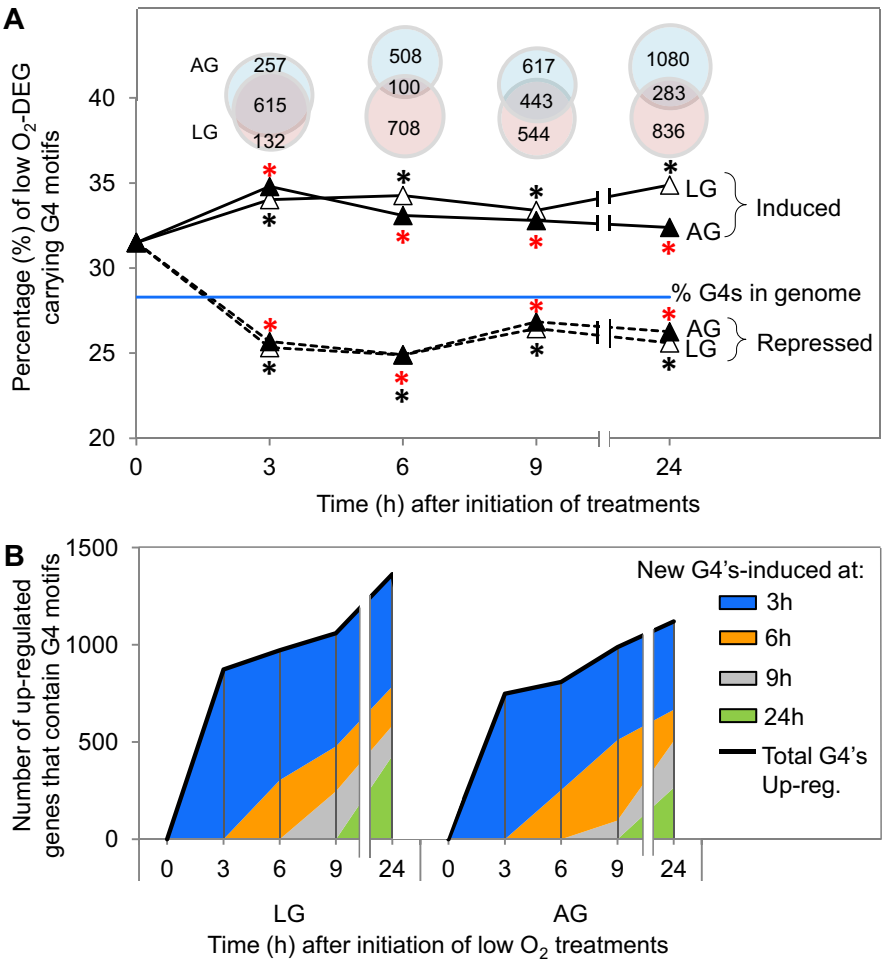

Figure 5 Responses by hypoxia-regulated genes over time, which carry motifs with potential to form four-stranded, DNA-quadruplex structures (G4s). (**A**) Proportion of G4 motifs among the total number of DEGs under low oxygen in LG (0.2% w/v) or AG (2% w/v). The probability of the observed frequency for G4-motifs in a DEG set (induced or repressed) occurring by random chance was determined using a binomial distribution test where n = total number of DEG at each time point, k = number of DEG's that contain G4s at each time point, p = proportion of G4-containing genes in the whole maize genome (28%, blue line), and q = 1–0.28. Asterisks indicate where the probability was significant ($P < 0.05$) for DEG in low (black) or abundant (red) glucose. (**B**) Number of G4-containing genes that were newly upregulated at each time point.

G4 responses depending on glucose availability (Figure 5A, Venn diagrams above time-course; Supplemental Dataset S3).

In addition, many of the initial, sugar-independent transcripts were later displaced by the slower, sugar-modulated mRNAs, such that by 24 h, the latter accounted for over half of the total upregulated G4 genes (Figure 5B). Among these, when glucose was abundant, we consistently observed a significant representation of G4-containing genes in GO categories associated with carbohydrate metabolism (Supplemental Figure S4). Finally, evidence here also shows that hypoxia increases the number of starvation-induced genes (Figure 1, B and 5, A), so together with the above, data collectively indicate that G4-containing genes are not only regulated by hypoxia, but also by sugar availability.

GO-term analysis also showed a significant enrichment of transcripts associated with regulation of transcription and hormone metabolism (Supplemental Figure S4). Possible roles for G4-motifs are thus suggested in genes for gibberellins (GAs) and other hormones under low-oxygen conditions.

Oxygen levels alter metabolite profiles for sugars and respiratory intermediates

Due to enhancement of core hypoxic responses by the glucose-depletion observed above (Figures 3 and 4, B), we sought to characterize endogenous sugar levels using targeted-metabolite profiling (Figure 6; Supplemental Figure S5). At the time of excision (0 h), glucose was the predominant sugar in root tips with levels 2-fold greater than fructose and 30-fold more than sucrose (Figure 6, A and 6, C). Within 6 h, these glucose levels had risen still further if aerobic roots were supplemented with physiologically AG. Under these conditions, glucose content increased two-fold, as did that of fructose, but sucrose abundance rose five-fold. The sucrose accumulation indicated that aerobic roots can use

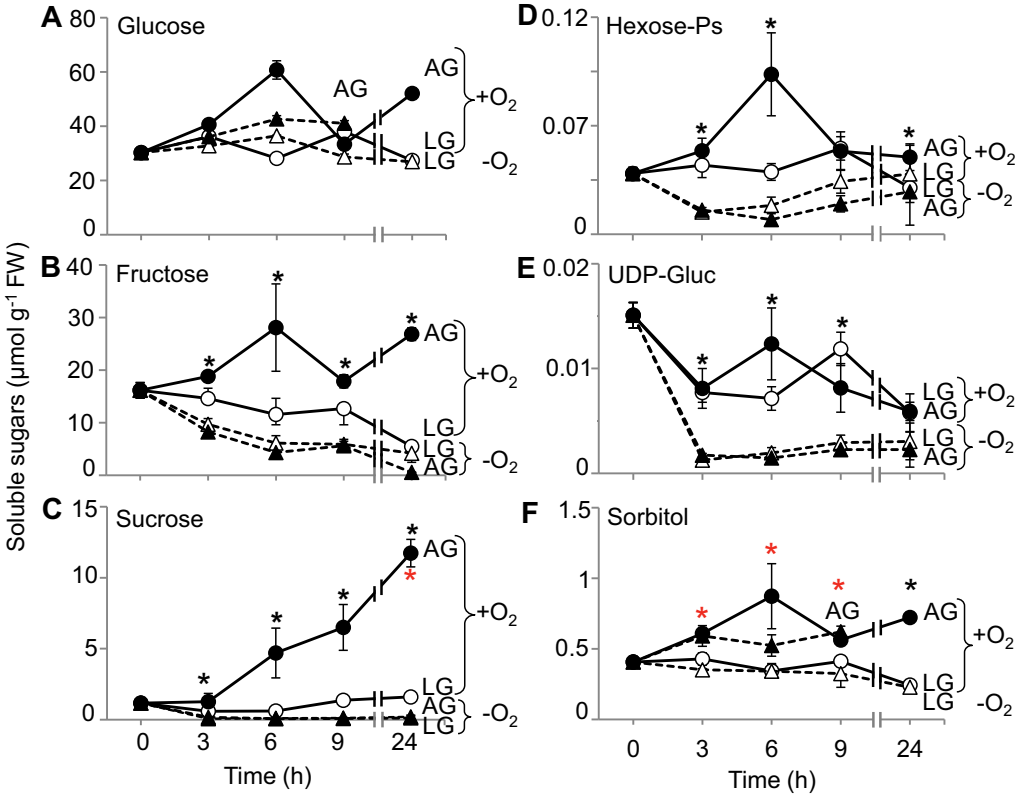

Figure 6 Profiles of sugars and their primary metabolites in roots exposed to different levels of oxygen and sugars over time. Metabolite levels throughout the treatments were quantified by GC-MS (**A–D**) or LC–MS–MS (**E** and **F**). Treatments included two oxygen levels: ambient air (+ O_2; 21% O_2 v/v) or low oxygen (−O_2; 0.2% O_2 v/v) in combination with two glucose concentrations: LG (0.2% w/v) or AG (2% w/v). Data represent mean values ± SEM; $n = 3$. Asterisks indicate a significant difference in responses to oxygen concentrations (black) or between glucose levels (red) according to two-way ANOVA ($P \leq 0.05$).

glucose to synthesize sucrose, which is consistent with abundant sucrose synthase and enhanced levels of *Spp* and *Sps* mRNAs described above (Figure 4D).

Under hypoxia, however, no sucrose accumulation was detectable regardless of glucose supplies. Endogenous sucrose was depleted between 3 and 6 h of low oxygen (Figure 6C). Fructose levels also dropped rapidly, with less than half the original amounts remaining after 6 h, again regardless of glucose supplies (Figure 6B). In contrast, glucose levels remained relatively unchanged in hypoxic roots, even without exogenous additions (Figure 6A). The lack of sucrose accumulation under low oxygen was not countered by the upregulation of mRNAs for *Sps* and *Spp* under these conditions. Although transcriptional mechanisms for sucrose biosynthesis may be in place, (1) the process may be limited at other levels of control and/or (2) sucrose may not accumulate due to rapid use. The latter is supported by the speed of depletion observed above for endogenous sucrose pools, and also by indications of active sucrose cycling in maize roots even during hypoxia (Alonso et al., 2005, 2007).

Hypoxia and sugar supplies had variable effects on intermediates of central metabolism. Size of the UDP-glucose pool, for example, dropped precipitously in the first 3 h of hypoxia, regardless of glucose availability (Figure 6E). Results were consistent with a rapid shift to the sucrose synthase path of glycolysis initially implicated for sugar-starved plant cells by Huber and Akazawa (1986). Here, levels of hexose-P decreased slowly under hypoxia (Figure 6D) and could have resulted from either reduced production of these ATP-costly intermediates, their rapid use, or both. In contrast, sorbitol abundance was minimally responsive to low oxygen and instead, closely paralleled fluctuations in pool size for endogenous glucose and fructose (Figure 6F).

Only modest changes were observed for levels of the glycolytic intermediate 3-PGA in any of the treatments examined (Supplemental Figure S5). Pools of citrate and malate were significantly lower during hypoxia compared to ambient air. At the same time, succinate levels initially rose, especially in sugar-depleted, hypoxic roots. In addition, ratios of NAD(P)H/NAD(P) were reduced (Supplemental Figure S5). Profiles of these metabolites reflect an expected downregulation of TCA-cycle activity and enhancement of alternate pathways (Narsai et al., 2011; Ramirez-Aguilar et al., 2011).

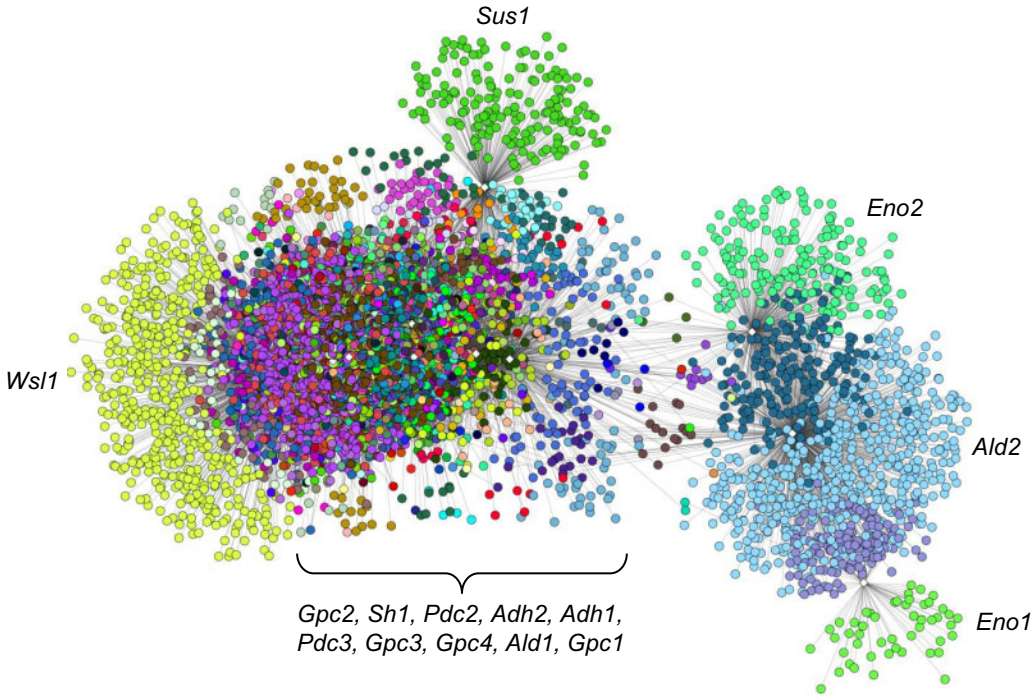

Figure 7 Co-expression network of genes for core ANPs. The co-expression network was constructed using 15 genes coding for ANPs (designated by Sachs et al. (1980); Supplemental Table S4) as baits. Co-expressed targets were identified in the transcriptome data from 60 different RNA-Seq libraries, each representing responses of 0.6-cm maize root tips under either aerobic (21% O_2 v/v) or low-oxygen conditions (0.2% O_2 v/v) using CoExpNetViz (Tzfadia et al., 2016). Data were analyzed using the Pearson correlation co-efficient, with the 5 lowest and 95 uppermost percentile rankings as thresholds for co-expression. Dots with the same color represent genes co-expressed with a given bait, based on positive correlations where $R^2 > 0.8$. For gene identifiers, see Supplemental Table S1. *Wsl1*, Receptor-*like protein kinase-related*.

Co-expression networks for core hypoxia genes are dynamic and sugar-responsive

To identify functional and organizational patterns in gene expression over time and under different conditions, we constructed and analyzed a guided co-expression-network beginning with mRNAs for 15 ANPs (Supplemental Table S1). Relationships were identified using the Pearson correlation co-efficient, with the 5 lowest- and 95 uppermost-percentile ranks to define thresholds for co-expression. Since, ANP genes are selectively transcribed and translated during hypoxia (Sachs et al., 1980; Mustroph et al., 2009), we used these genes as baits to focus on mRNA targets with positively correlated expression ($R^2 > 0.8$). The resulting network included 5,733 nodes (transcripts) and 26,348 edges, which collectively revealed two major connected components (Figure 7). One large component was composed of most of ANP bait genes and their targets while the second component included three bait genes: *Enolase1* (*Eno1*), *Enolase 2* (*Eno2*), and *Aldolase 2* (*Ald2*). Distinct coordination of expression was thus indicated for the second component of the network compared to most bait genes. To determine the sugar-responsiveness of these networks and extent of transcriptional coordination within and between them, we paired the core ANP network with transcriptome profiles for DEGs under each condition tested here.

Two sets of co-expression networks were defined under low-oxygen conditions; one from limited glucose (LG); and one from AG (Figure 8). Over the entire 24-h period, a greater number of genes (nodes) were significantly co-expressed with the ANP bait genes when glucose was abundant (Figure 8). Under these conditions, network size increased over time, with average number of neighbors per node rising from 6 at 3 h to 9 at 24 h. However, network size was actually greater during initial responses to hypoxia by low-glucose root tips, but later decreased. The average number of neighbor genes increased during the first 9 h of hypoxia from 8 at 3 h to 10 at 9 h, but dropped to 2 after 24 h of low oxygen. Similarly, the clustering coefficient, a measure of local connections in the networks (Horvath and Dong, 2008) varied depending on glucose availability. When glucose was abundant, clustering coefficients in ANP-centered networks increased throughout the experiment from 0.54 to 0.65, but low glucose led initial increases in these values to decline from 0.61 to 0. This measure of clustering further defined the capacity for glucose to maintain and increase the size of co-expression networks under prolonged hypoxic conditions. Nonetheless, the magnitude of initial low-oxygen responses at the gene network level was greater when glucose supplies were limited.

Subsequent analysis of the ANP-related networks with low and abundant glucose supplies (LG and AG) identified highly interconnected regions that included *Adh*, *Pdc*, *Sh1*, *Phosphohexose isomerase 1* (*Phi1*), and *Wusl1032* (Supplemental Figure S6). The topological properties and

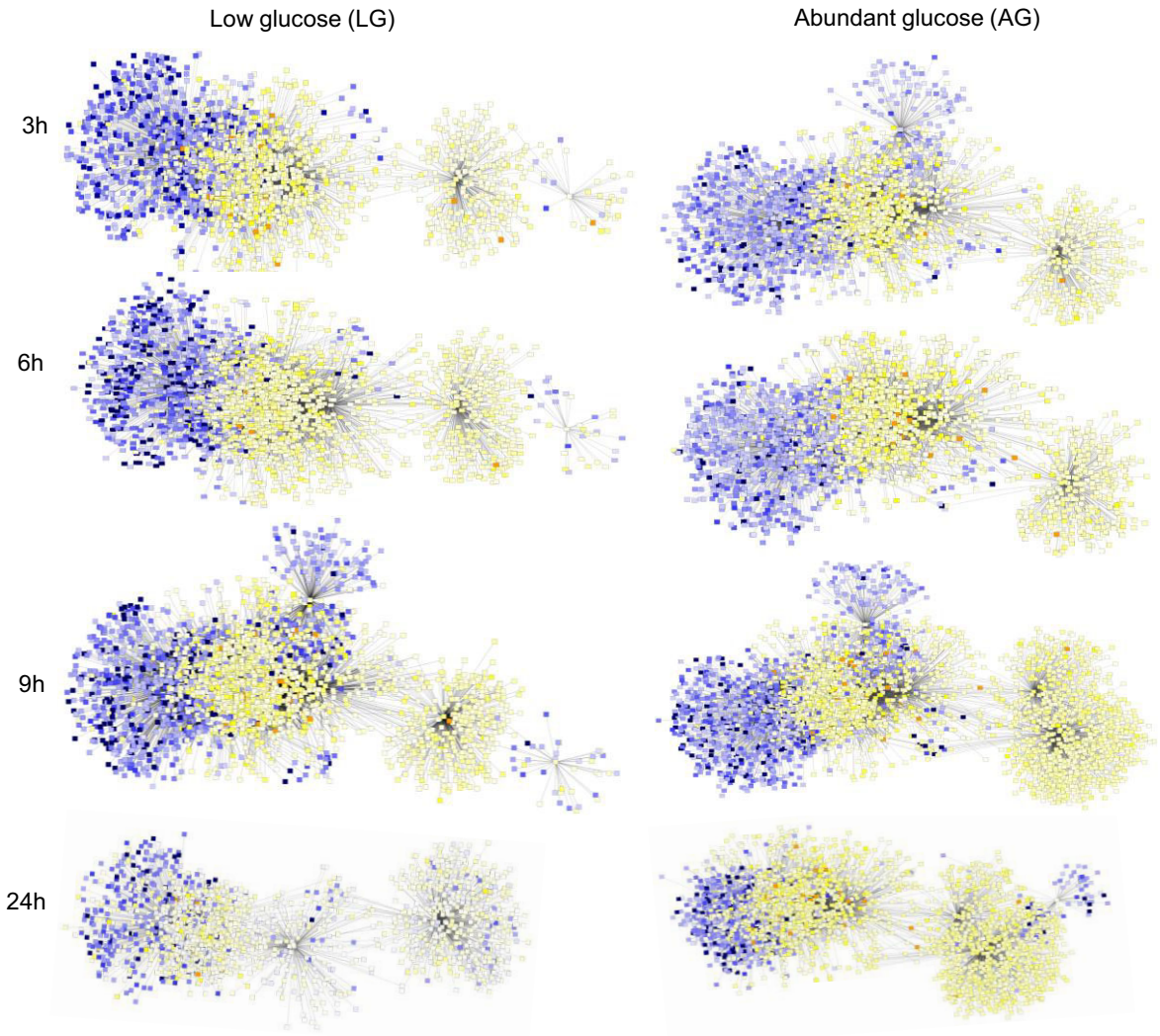

	LG				AG			
Time (h)	3	6	9	24	3	6	9	24
Number of nodes	2584	2903	3298	2151	2772	2825	4073	3618
Number of edges	10260	11800	16222	2158	8219	8829	15946	16568
Clustering coefficient	0.613	0.594	0.585	0	0.54	0.5	0.539	0.647
Average no. of neighbors	7.941	8.13	9.837	2.01	5.9	6.25	7.83	9.159

Figure 8 Changes in the co-expression network of genes for core ANPs throughout oxygen and sugar treatments in maize. The overall network is as shown in Figure 7, modified here with altered color to show regulation of component genes and changes in their co-expression relationships in each glucose concentration: LG or physiologically AG. Visualized data represent target genes that were positively correlated ($R^2 > 0.8$) and differentially expressed ($P < 0.05$). Downregulated genes are shown in blue, with strongly downregulated genes (more than two-fold) in black. Upregulated genes are shown in yellow, with strongly upregulated genes (more than two-fold) in orange. The Table shows topological characteristics of co-expression networks among low-oxygen-responsive genes under each glucose condition.

co-expression relationships of these clusters changed over time depending on glucose availability, indicating that the extent of transcriptional coordination is dynamic. Overall, modules with *Adh* genes were small and clustered together with only a few others. Clusters with *Sh1*, on the other hand, were composed solely of the other ANP bait genes (Supplemental Figure S6). Among the modules identified, those consisting of *Pdc3* and *Gpc4* had the densest neighborhoods and grew most steadily over time (Figure 9A). Further analysis of these *Gpc4–Pdc3* networks showed that glucose altered the identity of all co-expressed genes detected (Supplemental Dataset S4), thus restructuring these central modules by introducing an essentially all-new set of interrelationships and co-expression partners over time.

Enrichment analysis of co-expressed genes in the *Gpc4–Pdc3* modules under low glucose revealed that many were related to regulation of cellular and biological processes, protein binding, and reproductive development

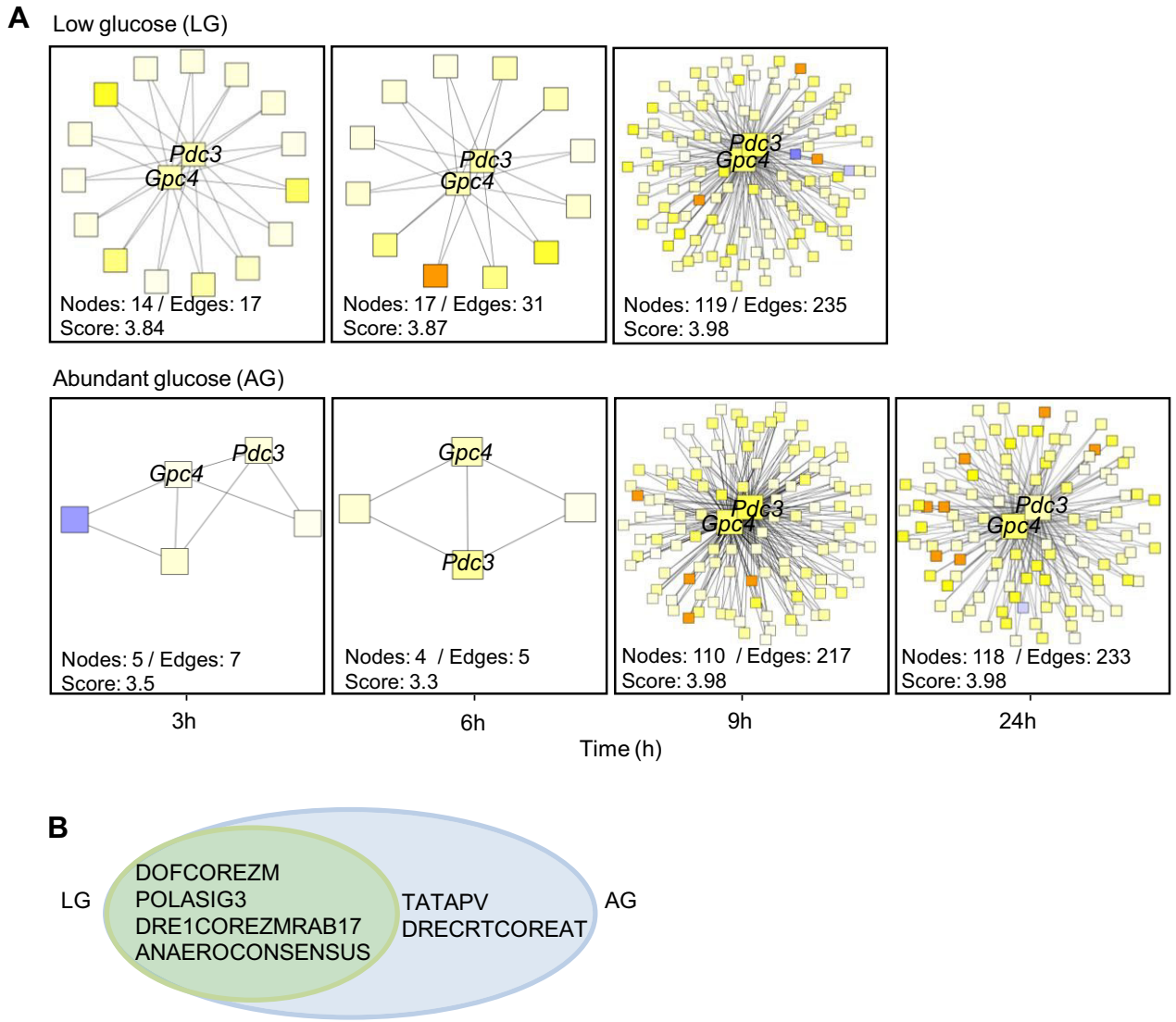

Figure 9 Modules of the most highly interconnected co-expression networks for genes expressed under low-oxygen with either AG (2% w/v) or LG (LG; 0.2% w/v) levels. (**A**) Modules were identified using the Cytoscape MCODE algorithm plug-in. Nodes represent DEG ($P < 0.05$) and edges represent significant co-expression between DEG. Color indicates expression levels: blue (downregulated); yellow (upregulated); orange (more than two-fold upregulated). (**B**) *Cis*-regulatory elements identified in co-expressed members of the *Gcp4–Pdc3* modules. Promoter sequences were analyzed using the PlantPAN2.0 (Chow et al., 2015). Partners in these modules shared four of the motifs noted when glucose was limiting (LG, green oval), but only two where distinct to module genes when glucose was abundant (AG, blue oval).

(Supplemental Table S2). When glucose was abundant, upregulated genes included several associated with sugar metabolism, glycolysis, transport, protein modification, and nucleic acid binding. Later, at 24 h, mRNAs also included genes for reproductive development and others for regulation of biological processes and responses to stimuli (Supplemental Table S2).

To further define the glucose-dependent contrast in composition of the *Gpc4–Pdc3* modules, we screened the promoter regions of co-expressed genes for common *cis*-regulatory elements. We found that for each glucose level, there were mutual elements regulating transcription of co-expressed genes in the *Gpc4–Pdc3* modules (Figure 9B). Two additional elements (TATAPVTRNLEU and DRECRTCOREAT) were distinctive among members of abundant glucose modules. Moreover, the set of *cis*-elements identified varied over time, indicating their relevance to module regulation and message stability during rapid and longer term responses to hypoxia. Together these results revealed specific contributions of sugars to co-expression relationships between low-oxygen transcripts.

Discussion

Responses to hypoxia are being carefully studied at multiple levels in both rice and Arabidopsis (van Dongen and Licausi, 2015; Gasch et al., 2016; van Veen et al., 2016; Locke et al., 2018; Cho et al., 2019). However, the extent and mechanisms of sugar interface with hypoxic responses have been difficult to distinguish beyond the earlier work of

Loreti et al., 2005 and Lasanthi-Kudahettige et al., 2009. In the first of these studies, microarray analyses focused on whole Arabidopsis seedlings incubated in an oxygen-free environment for 6 h with or without sucrose. Later, Lasanthi-Kudahettige et al., 2009, characterized transcriptome modifications of rice coleoptiles under aerobic and anaerobic conditions, including the low-oxygen induction of a starvation-responsive-*AMY3D* gene for α-amylase. Here, our purpose was to define sugar-modulated components of the whole-genome response to low-oxygen conditions. We hypothesized that reconfiguration of the transcriptome under hypoxia would involve a combination of sugar-responsive genes as well as other mRNAs essentially insensitive to sugar availability. We further expected that the balance between these inputs would shift during progression of the low-oxygen response and that in-depth analysis of the sugar–oxygen interface could lead to new insights into underlying regulatory mechanisms.

Toward these ends, we first characterized the overall framework and timing for the hypoxic response in a maize root-tip system where both oxygen and sugar levels could be precisely controlled. Glucose was used for this work, partially because it normally predominates in maize root tips (Figure 6; Dieuaide-Noubhani et al., 1995; Bouny and Saglio, 1996; Alonso et al., 2005). In addition, early studies indicated that apoplastic transport of sucrose into maize root tips typically involved hydrolysis into hexoses in the cell-wall space (Guiaquinta et al., 1983). Moreover, symplastic transport alone, without exposure of sucrose to cell-wall invertases, is insufficient to satisfy estimated carbon demands for growth of maize root tips (Bret-Harte and Silk, 1994). Subsequent work by Bouny and Saglio, 1996 showed that responses of excised maize roots supplemented with exogenous sucrose were similar to those incubated with glucose or fructose, presumably due to action of the extracellular cell-wall invertase. Use of glucose in the present work thus provided the most direct path of entry into central metabolism. The concentrations used were based on those previously found to support root respiration and accumulation of mRNAs for sugar metabolism (Saglio and Pradet, 1980; Koch et al., 1992). Root tips in this system grew rapidly if ambient air was provided, and remained responsive to markers of sugar and oxygen status (Supplemental Figure S1).

Oxygen-responsive mRNAs include sugar-modulated genes

The root-tip system and time course used here provided the framework for more in-depth dissection of transcriptional reconfiguration that occurred when sugars, oxygen, or both were either limiting or abundant (Figure 1; Supplemental Figure S2). Results allowed identification of feast and famine contributions to hypoxic responses and a determination of extent and timing for this input (Figure 1; Supplemental Tables S1 and S2). Regardless of sugar availability, 3 h of hypoxia induced major restructuring of the maize root-tip transcriptome (Figure 1A). The speed and extent were comparable to the rapid changes in transcript, protein, and metabolic profiles observed within 0.5 to 6 h of hypoxia for Arabidopsis seedlings (Loreti et al., 2005; van Dongen et al., 2009; Lee et al., 2011; Mustroph et al., 2014; Locke et al., 2018). In terms of gene numbers affected, the widespread repression observed here under hypoxia was expected, whereas the combination of up- and downregulated mRNAs from glucose deprivation was less so (Figure 1, B and 1, C). Earlier work with Arabidopsis had indicated that sucrose could reduce the extent of hypoxia response after a 6-h low-oxygen treatment, whereas starvation would reduce expression of hypoxic genes after 12 h of dark hypoxia (Loreti et al., 2005, 2018; Cho et al., 2019, 2021). Here, our time-course analysis of the maize root-tip system revealed that the hypoxic transcriptome included an increasing compliment of sugar-repressible, starvation-enhanced genes over time (Figure 1, B and C).

Among such genes is the prominent group of those encoding core hypoxic genes or ANPs (Sachs et al., 1980; Mustroph et al., 2009). Although their induction is partially regulated by the stabilization of the ERF-VII-family of transcription factors, sugar availability has long been recognized as a key contributing factor of their modulation during hypoxia (Koch et al., 1992; Zeng et al., 1998, 1999; Loreti et al., 2005; Cho et al., 2019, 2021). For the majority of ANPs, starvation had a pronounced effect as indicated by the greater levels of these mRNAs when glucose supplies were limited (Figure 3). The differential regulation by oxygen and sugars of different ANP isoforms included the two main sucrose synthases: *Sh1* and *Sus1*. Our data are consistent with previous work (Koch et al., 1992; Zeng et al., 1998) indicating that *Sus1* levels were maximal in hypoxic high sugar environments, while *Sh1* was highly induced by anoxia and starvation. The sugar treatments employed here were comparable to those used in other studies, and the transcript profile of *Sus1* and *Sh1* in response to sugar levels was equally consistent. Our results also indicate that the hypoxia treatment used here was severe, since *Sh1* levels were higher than those of *Sus1*, especially after prolonged exposure with LG supplies (Figure 4B). In low-oxygen conditions, the preferred accumulation of sucrose synthase over invertase (Figure 4B) would theoretically be an energetic advantage at a local level given that invertase-mediated sucrolysis has a two-fold greater demand for ATP compared to the one UTP and inorganic pyrophosphate used for the sucrose-synthase path of breakdown. The relatively minimal levels of invertase mRNAs compared to those of sucrose synthase (Figure 4B), even under aerobic conditions, are consistent with a predominantly sucrose-synthase path for sucrose cleavage in maize root tips.

At the GO level, abundant glucose had a significant effect on hypoxic responses in categories associated with "ribosome biogenesis" and "formation and elongation of polyribosomes" (Figure 2). These categories represent energy-demanding processes strictly dependent on cellular ATP and sugar availability. The representation of these GO terms may reflect operation of the translational machinery poised to

translate selective mRNAs for ANPs and other sugar- and/or oxygen-responsive genes. This possibility is consistent with the sugar-dependent enhancement of polysome loading, ribosome associations, and chromatin accessibility of genes for carbohydrate metabolism and fermentation during hypoxia (Pal et al., 2013; Gamm et al., 2014; Lee and Bailey-Serres, 2019; Reynoso et al., 2019). In maize root-tips, glucose abundance and prolonged hypoxia beyond 6 h also led to increase in the number of transcripts associated with RNA/protein synthesis. The significant over-representation of these transcripts indicates a distinctly positive effect of glucose at the mRNA level even under hypoxia. Though steady-state mRNA levels may or may not correspond to the extent of translation (Branco-Price et al., 2008; Juntawong et al., 2014), sugars can also affect the latter, even when oxygen is limiting. In mammalian cells, for example, glucose additions can transiently counter repression of translation during hypoxia (Thomas et al., 2008). In plants, sugar signals mediated by SnRK1 enhance translation efficiency of mRNAs for acclimation to hypoxia, while in yeast (*Saccharomyces cerevisiae*), glucose availability and the TOR-complex1 (TORC1) regulate expression of ribosomal genes that enhance survival and regrowth after C-starvation (Branco-Price et al., 2008; Xiong et al., 2013; Juntawong et al., 2014; Cho et al., 2019; Morgan et al., 2019; Parenteau et al., 2019). Each of these examples indicates that both low-oxygen and sugar status can modulate translation in those systems.

Results here thus reveal that sugars modulate the accumulation of specific mRNAs for ANPs and also the extent to which transcriptome profiles respond to hypoxia. Moreover, the effect of C-supplies extends beyond transcriptional reconfiguration for metabolic paths to those associated with ribosome function and post-transcriptional processes.

G4 motifs are prevalent in genes associated with hypoxia, starvation, and hormone metabolism

G4 motifs have emerged as important components of low-oxygen responses at different levels of regulation in eukaryotes (Clark et al., 2012; Welsh et al., 2013; Fedeles, 2017; Fleming et al., 2017), and potential roles of G4s in plants are attracting increased interest (Andorf et al., 2014; Cho et al., 2018; Griffin and Bass, 2018). Here, we evaluated the previously unexplored regulatory potential of G4-motifs and the dynamics of G4-gene expression during low-oxygen and C-starvation stresses. Recent work in maize has indicated that G4 sequences are abundant in genes associated with low-oxygen, starvation, and oxidative stress (Andorf et al., 2014). We thus hypothesized that G4 genes would be enriched among those upregulated by hypoxia. Analysis confirmed that this was indeed the case (Figure 5A; Supplemental Dataset S3). Although glucose availability had little effect on the total number of G4 genes induced under low oxygen, a comparison of profiles showed that first-responders (3 h) were essentially sugar-independent, whereas later inductions (after 6 h) were sugar-modulated (Figure 5A). A key feature of G4 motifs is their suggested capacity to "poise" transcriptional machinery for rapid responses to severe stresses. For this reason, we had expected many of the G4-gene responses to occur rapidly, as was evident at the gene-number level (Figure 5A). However, analysis of individual genes showed that new G4 genes were continuously induced during the 24-h low-oxygen treatment. Moreover, these newly expressed genes were enriched for sugar-modulated mRNAs that eventually comprised over half the total G4 genes upregulated by hypoxia.

Timing of change in the G4-gene profiles (Figure 5A) indicated that glucose-responsive G4s could become increasingly important contributors to acclimation responses after the initial 6 h of low-oxygen signals, during periods when changes in sugar availability and related metabolism become more prominent. The 6-h timepoint is indeed when the greatest shifts in sugar levels and metabolites emerged in this root-tip system (Figure 6; Supplemental Figure S5). In addition, sugars play a role in the physical stability of G4 structures, while both sugars and G4s can regulate mRNA half-life and maturation (Chan and Yu, 1998; Beaudoin and Perreault, 2013; Gómez-Pinto et al., 2013; Cho et al., 2018). These impacts of both sugar and oxygen on the dynamics of G4 genes could provide a mechanism that aids the coupling of gene expression with metabolic status during the progression of hypoxic responses over time. In mammalian systems, for example, the eukaryotic initiation factor A (eIF4A; a component of the eIF4F protein complex that regulates translation) can bind and unwind G4 structures in mRNAs (Wolfe et al., 2014; Song et al., 2016). This interaction between eIF4A and G4s allows translation of selective mRNAs by eIF4G. Remarkably, in plants, eIF4G phosphorylation by SnRK1 enhances translation of mRNAs for hypoxia responses including those for *Adh* (Cho et al., 2019, 2021). These observations, together with data presented here, indicate at least one potential mechanism by which G4 motifs can contribute to oxygen and sugar signals. Although roles may be diverse, work here shows that G4 elements and their host genes are prominent components of the low-oxygen response in plants.

Additional investigation of hypoxia-responsive G4 genes at the GO-term level indicated an enrichment of G4 sequences in genes for hormone responses, especially GA (Supplemental Figure S4). The G4 motifs could be relevant through direct or indirect integration of signaling pathways under hypoxia. For instance, transcriptional regulation of GA signals during low oxygen can define escape or quiescent strategies for flooding tolerance in rice (Fukao and Bailey-Serres, 2008; Colebrook et al., 2014). Furthermore, in flooded soybean (*Glycine max* L.), GA plays a significant role in ROS homeostasis and nitric oxide (NO) signaling (Khan et al., 2018). Collectively, our data support possible roles for G4 motifs in hormonal responses to low oxygen, and also to diverse, starvation-independent components of the hypoxic transcriptome.

Metabolite profiles were consistent with shifts in sucrose cycling even under hypoxia

Impacts of sugar and oxygen availability on targeted-metabolite profiles (Figure 6; Supplemental Figure S5) were compared to simultaneous remodeling of the transcriptome, plus known effects at the protein level (Sachs et al., 1980; Mustroph et al., 2009). Resulting integrations showed that levels of endogenous sucrose and hexoses rose as long as both oxygen and glucose were abundant (Figure 6). A clear capacity for maize root tips to synthesize sucrose is evident in these data and further supported by previous work on preferential sucrose use as a metabolic substrate in maize roots fed exogenous glucose or fructose (Bouny and Saglio, 1996). This sucrose can be re-synthesized from either the products of previous sucrose cleavage or exogenously fed hexoses. A similar re-synthesis is also central to development of maize kernels, where sucrose in route to starch storage in the hypoxic endosperm is initially cleaved in the extracellular space of the pedicel, then re-synthesized before final use (Shannon, 1972; Alonso et al., 2011). This cycling (cleavage and re-synthesis) of sucrose in maize roots is estimated to mediate a major flux during primary metabolism (Dieuaide-Noubhani et al., 1995; Alonso et al., 2007). Transcriptome data here (Figure 4D) indicate that sucrose synthesis (or re-synthesis) could potentially be mediated by either the reversible sucrose synthase reaction or the SPS–SPP path (sucrose-P synthase + sucrose-P phosphatase), both abundantly represented at the mRNA level. Once formed, this sucrose is the likely source of the free fructose observed in the present work (other nonsucrose paths to free fructose remain equivocal). Both known paths of sucrose cleavage produce a free-fructose product (invertase and the reversible sucrose synthase). Consistent with a sucrose source for the fructose in these root tips is the observation that fructose pool size was maintained only when sucrose was abundant and declined steadily otherwise (Figure 6B). The alternative production of free hexoses from futile cycling of hexose-P would require a hypothesized hexose phosphatase (Dieuaide-Noubhani et al., 1995; Alonso et al., 2005). However, despite evidence for the activity of a putative glucose-6-phosphatase in plants, this enzyme remains unidentified (Alonso et al., 2005; Claeyssen and Rivoal, 2007).

Low oxygen severely reduced levels of most sugars in maize root tips except for glucose and sorbitol (Figure 6, A and 6, F). The sucrose pool was nearly depleted within the first 3 h of hypoxia, a response comparable to that observed elsewhere with anaerobic roots (Bouny and Saglio, 1996; Germain et al., 1997; Mustroph and Albrecht, 2003). This observation was expected given the preferential use of sucrose noted above for hypoxic maize roots regardless of which exogenous sugars are provided (Bouny and Saglio, 1996). Despite the probable constraint to ATP supplies, metabolic modeling in maize roots has indicated that sucrose cycling could continue under hypoxia and would depend on extent of available ATP (Alonso et al., 2007). If so, then even the small sucrose pool observed here would be concurrently supplying both glycolysis and its own cycling. Such a scenario is consistent with the hypoxic induction of transcripts for sucrose synthase, SPS, and SPP seen here (Figures 2, A and 4, D). Moreover, glucose incorporation into sucrose follows a path that requires hexose-P and UDP-glucose. Both these metabolite pools were significantly reduced by low oxygen, and their decrease over time approximately paralleled that of sucrose (Figure 6, D and Figure E).

The suggested cycling of sugar metabolites in a low-oxygen environment by Alonso et al. (2007) seems initially contradictory given the extent to which acclimation strategies favor conservation of ATP. Theoretically, futile cycles may increase flexibility of plant metabolism by allowing a rapid change in the direction of net flux while maintaining balanced ratios of ATP and ADP (Dieuaide-Noubhani et al., 1995; Hill and ap Rees, 1995; Alonso et al., 2005, 2007). For instance, in yeast cells, $>40\%$ of excess glucose is stored as readily available energy in the form of glycogen and trehalose (Shulman and Rothman, 2015). Synthesis of these metabolites helps maintain homeostasis of ATP and glycolytic intermediates in aerobic- high-glucose environments (Shulman and Rothman, 2015). Although mechanisms vary, the yeast trehalose/glycogen shunt would be analogous to the accumulation of sucrose observed here and its suggested cycling in maize roots. In these systems, sugar accumulation could provide a centrally important means of maintaining metabolic homeostasis during large changes in glucose availability. Our data provide additional support for this hypothesis given that synthetic capacity of glucose would depend on the phosphorylating activity of HXK. We observed an accumulation of *Hxk* mRNA (Figure 4B) consistent with the sustained activity of HXK reported during hypoxia by Bouny and Saglio, 1996.

Data here also indicate that mechanisms other than fermentation contribute to the recycling of NAD^+. First, sorbitol accumulated to a greater extent in roots supplemented with abundant glucose (Figure 6F). Sorbitol is formed during the NADH-dependent reduction of fructose by sorbitol dehydrogenase (SDH) and the generation of NAD^+ (de Sousa et al., 2008). In some respects, the low-oxygen, high-sugar treatment used here has similarities to that of the maize endosperm, where the SDH pathway is active and proposed to aid redox balance and maintenance of energy status (de Sousa et al., 2008; Gayral et al., 2017). Second, roots in low oxygen had lower ratios of NAD(P)H/NAD(P) than those in ambient air (Supplemental Figure S5). Depletion of NAD(P)H during hypoxia has been associated with futile cycling of nitric oxide (NO; Dordas et al., 2003). This cycle produces $NAD(P)^+$ that can sustain glycolytic flux, while at the same time, NO levels contribute to oxygen signals by modulating the N-end-pathway of protein hydrolysis (Igamberdiev and Hill, 2004; Gibbs et al., 2014; van Dongen and Licausi, 2015). Lastly, succinate accumulation, together with decreases in citrate and malate levels (Supplemental Figure S5), are consistent with expected downregulation of the TCA cycle and use of alternative respiratory substrates for ATP production (Rocha et al., 2010; van Dongen et al., 2011; Antonio et al., 2016).

Sugar availability alters co-expression relationships of ANPs in prolonged hypoxia

Sugar-modulated components of hypoxic responses were clearly apparent in gene-expression networks constructed from a core of maize ANPs (Figure 7; Supplemental Table S1). These networks showed prominent effects of glucose supplies on topological properties, including an enhancement of network size, density, clustering coefficients, and connectivity (Figure 8). In general, the number of differentially co-expressed genes was similar, but the interconnections between them were markedly increased if glucose was present during prolonged periods of low oxygen (Figure 8). The greater number of nodes and extent of clustering showed that glucose enhanced the co-expression relationships associated with core hypoxic genes. The reverse was observed with glucose limitation, indicating that sugar supplies may be central for maintaining gene relationships during prolonged hypoxia. Results here thus revealed that sugars not only modulate mRNA levels of core ANP genes, but also play a role in maintaining their co-expression relationships. The shifting dynamics of these co-expression networks in response to sugars provide a potential mechanism for prioritizing primary metabolism and metabolic homeostasis under long-term hypoxia.

Topological analysis of co-expression networks identified several modules that persisted under hypoxia regardless of sugar levels. These were comprised mainly of *Adh*, *Pdc*, *Sh1*, *Phi1*, and *Wusl1032* (Supplemental Figure S6). Although these genes were highly interconnected with each other in the network and are central to the low-oxygen response of maize, they were not entirely coordinated at a transcriptional level. Our analysis shows that sugar level and duration of hypoxia altered their co-expression patterns. Only clusters containing the *Gpc4* and *Pdc3* were consistently co-expressed regardless of sugar levels (Figure 9A). Still, throughout the treatments, *Gpc4* and *Pdc3* shared co-expressed couplings that were distinct for each glucose level (Figure 9A; Supplemental Dataset S4). The strong relationship between these two bait genes and their targets indicates that sugar levels may trigger cooperative responses among these genes in response to altered oxygen status. Metabolically, this is particularly relevant, since *Gpc4* and *Pdc3* encode enzymes that, respectively, regulate the initial and final reactions of glycolysis. They are credited with controlling the rate of glucose catabolism and cycling as well as demonstrated roles in hypoxia acclimation (Sachs et al., 1996; Ismond et al., 2003).

A closer look at these *Gpc4–Pdc3* networks revealed that functional categories of transcripts in modules from low- and abundant-glucose treatments changed over time (Supplemental Table S2). The shifts observed were consistent with the importance of both sugar and oxygen input. The differential co-expression patterns observed here under feast and famine conditions correlated with *cis*-regulatory elements shared within modules. However, two additional elements were identified as distinctive to the transcriptome re-structuring that occurred under low oxygen when glucose was abundant (Figure 9B). One of these sequences, TATAPVTRNLEU, functions as a TATA-like motif in maize, where it allows binding of a Myb transcription factor that can enhance anaerobic expression, as observed for *Gpc4* (Geffers et al., 2001). This *cis*-element can also play a role in re-initiating transcription of plant tRNA genes (Yukawa et al., 2000). The second of these motifs, DRECRTCOREAT, is a dehydration-responsive element (Qin et al., 2004).

Using the *Gpc4–Pdc3* modules, we identified putative players associated with secondary signaling pathways that operate at different points in the sequential series of hypoxic responses. These networks and their partners represent new and potentially central aspects of sugar contributions to the progressive transcriptional responses under low oxygen. Furthermore, construction of gene-expression networks revealed initially unexpected roles of glucose availability in determining network partners for core-hypoxia genes.

Conclusions

The present work identifies and dissects previously unrecognized contributions by sugars to low-oxygen impacts on plants. The separation of transcriptional responses to sugar availability from those associated with hypoxia demonstrated that sugars modulate specific, oxygen-responsive gene networks without affecting others. Although impacts of hypoxia predominate in maize root tips, sugar supplies alter these responses in distinctive ways. Starvation stress enhances the magnitude and speed of initial transcript accumulation for ANP genes, whereas sugar abundance is central to maintaining co-expression relationships and network connectivity of ANPs under prolonged hypoxia. In addition, genes in co-expressed modules share a small set of *cis*-elements distinctive to their sugar status. Together, these co-expression networks define new roles of sugars in adaptive responses to low oxygen that extend beyond modulating mRNA levels for ANP genes. Results here also show that hypoxic induction of genes with G4-quadruplex motifs can be divided into two phases, the first one being fast and sugar-independent, the second one being less rapid, but modulated by feast-or-famine signals. Analyses of the collective inputs provided here reveal new components of low-oxygen responses and provide targets for rational approaches to enhancing hypoxia tolerance.

Materials and Methods

Plant material

Maize (*Zea mays* L.) seeds of the W22 inbred were surface sterilized for 15 min in 15% (v/v) sodium hypochlorite and rinsed with distilled water five times to remove traces of the hypochlorite. To ensure uniform seed germination, seeds were imbibed overnight at 25°C in distilled water shaking at 165 r.p.m. to allow oxygenation. After imbibition, drained seeds were germinated in darkness at 25°C on moistened germination paper in $25 \times 5 \times 39$-cm glass pans. Each pan was sealed and supplied with a continuous, humidified air flow at 1 L min^{-1} during the 3-d germination period. The

terminal 6-mm tips of primary roots were excised in distilled water to maintain tissue moisture until oxygen and sugar treatments were applied.

Flow-through system

Excised root tips of 3-d-old seedlings were used for four different experimental treatments: The two glucose treatments were physiologically abundant glucose (2% w/v [10 mmol]) or low glucose [0.2% w/v [1 mmol]), and the two oxygen treatments were ambient air (21% v/v) or low oxygen (0.2% v/v).

Root tips were incubated in Whites media for 24 h shaking at 85 r.p.m. on a compact digital mini rotator shaker. Hypoxia treatments were initiated using an established protocol described by Zeng et al. (1998). Briefly, root tips were exposed to a positive pressure and gas flow of 1 L min^{-1} and maintained for hypoxic (0.2% O_2 in N_2) or aerobic (ambient air, 21% O_2) treatments. Each source was fully humidified prior to chamber entry.

A subset of 12 root tips was sampled prior to initiation of treatments, weighed, and frozen in liquid N_2. These constituted pre-treatment controls for subsequent qPCR, RNA-seq, and metabolite analysis. Time-course samples were harvested after 3, 6, 9, and 24 h of treatment. Each was frozen in liquid N_2 and stored at −80°C until analysis. For each time point, including the 0-h pretreatment samples, there were three biological replicates. Each replicate consisted of 12 root tips (approximately 0.1 g total).

RT-qPCR

RNA was extracted using an RNAeasy Plant Mini Kit (Qiagen) and treated with DNase. Complementary DNA was made by reverse transcription with random primers and RNase inhibitor. The qPCR reactions were done in a StepOne thermocycler using a relative quantification protocol (Čikoš et al., 2007) with SYBRGreen PCR Master Mix in a 20-µL reaction mixture with gene-specific primers and three technical replicates per sample. For validation of ANP gene expression, a SYBR® Green fluorescent dye-based Luna® Universal One-Step RT-qPCR kit (New England BioLabs) was used with a CFX Connect real-time PCR detection system (Bio-Rad). Reference genes included maize genes for *tubulin1*, *ubiquitin carrier protein*, and 18S rRNA. All primer pairs (listed in the Supplemental Table S3) were designed to span an exon–exon junction to reduce the possibility of genomic DNA detection and amplification. The relative expression of each gene was determined following the modified $\Delta\Delta C_t$ method (Pfaffl, 2001). For each reaction, 100-ng total RNA was used for templates. A standard curve (0.01–00 ng) was run for each target on the plate, and the PCR efficiency of each primer pair was calculated. The PCR efficiency of all primer pairs was within 100 ± 3%.

RNA-sequencing and analysis

Frozen root tissue was homogenized and total RNA extracted using Trizol© and the RNAeasy Plant Mini Kit (Qiagen) following the manufactures' recommendations. RNA quality and quantity were assessed spectrophotometrically and by agarose gel electrophoresis. Illumina cDNA libraries were constructed using the NEBNext Ultra RNA Library Prep Kit for Illumina (NEB). The cDNA libraries were sequenced using standard protocols for Illumina HiSeq (Illumina Inc.). Libraries were quantified using an Agilent Bioanalyzer.

Quality control of RNA-seq reads, manipulation, and analysis was conducted using the Galaxy framework (Afgan et al., 2018). TopHat2 (Kim et al., 2013) was used to align reads to the maize B73 reference genome (B73 RefGen_v4) allowing two mismatches. Gene transcript quantification was estimated using the HTSeq-count tool (Anders et al., 2015) with the union resolution mode. Normalized read counts and standardized gene expression were used to identify and compare the top 30 most responsive genes between treatments based on ANOVA test ($P < 0.05$). Differential gene expression analyses and significance of treatments on gene expression were estimated using the R package DESeq2 (Love et al., 2014). Genes were considered differentially expressed if their *P*-value was $\leqslant 0.05$.

Hierarchical clustering was conducted using average linkage based on Euclidean distance methods with the Partek Genomics suite software (Partek®). GO was analyzed for DEGs, and results were visualized using the Pageman platform (Usadel et al., 2006). The Wilcoxon rank sum test with the Benjamini–Hochberg correction test (Benjamini and Hochberg, 1995) was used to determine statistically significant ($P < 0.05$) changes between different functional classes of transcripts.

Metabolic profiling

For targeted metabolite analysis, soluble sugars and metabolic intermediates were extracted as described previously (Ma et al., 2014) with the following modifications. Frozen root tips were ground to a fine powder in liquid N_2, followed by transfer of 20 mg to a 0.6-mL volume of extraction media containing 7:3 (v/v) methanol–chloroform (−20°C) plus 300 pmols of PIPES (1,4-Piperazinediethanesulfonic acid) as an internal standard. Polar metabolites were extracted twice from the chloroform/methanol phase using ddH_2O (4°C), and the supernatants were pooled. The methanol/H_2O phase was evaporated to dryness with a speed vacuum concentrator and polar metabolites re-suspended in 200 µL ddH_2O. The resulting extract was filtered through 0.45-µm centrifuge tube filters (Costar Spin-X). Intermediate metabolites were analyzed via LC-MS/MS following the protocol from Arrivault et al., 2009. Quantification of soluble sugars from the extractions was performed as described by Lisec et al. (2006) on an Agilent 7980A series gas chromatography (GC) equipped with an Agilent 5977A single quadrupole mass spectrum detector (MSD). Dry extracts were derivatized sequentially with methoxyamine hydrochloride and *N*-methyl-*N*-trimethylsilyl-trifluoroacetamide. Parameters used for the GC were as follows: Helium carrier gas fixed at 16.477 psi, splitless injection, inlet temperature 220°C, injection volume 2 µL, and syringe washes with acetone and

hexane. Sample analytes were separated using an equipped DB-5 column (5%-phenyl)-methylpolysiloxane, 30 m length × 250 μm i.d. × 1 μm film thickness; Agilent Technologies, Santa Clara, CA, USA). Oven temperatures were programmed as follows: An initial 100°C was held for 4 min, then ramped up at a rate of 5°C min^{-1} to 200°C, followed by a ramp-down rate of 10°C min^{-1} to 300°C, where it was held for 10 min. The MSD was equipped with an extractor ion source and tuned for sensitivity and mass accuracy prior to sample analysis. Parameters for the MSD were maintained as follows: MSD transfer line temperature at 280°C, MS source temperature at 230°C, MS quad temperature at 150°C, a solvent delay of 7.50 min, and a mass scan range of 50–650 m/z with a threshold of 150. An Agilent MassHunter Workstation Acquisition (version, Agilent Technologies, Santa Clara, CA, USA) was used for data acquisition and Agilent's MassHunter Quantitative Analysis program was used for subsequent data processing. Spectral deconvolution was performed for each sample in the program by hand to achieve a list of compounds that were then validated based on comparing retention time and spectra to authentic standards. The most abundant nonconvoluted m/z ion fragment for each compound was used to integrate peak area. Integrated peaks were quantified by three additional m/z ion fragments that were required to match ratios observed in authentic standards. Soluble sugar concentration (μmol g^{-1} FW) was calculated using standard curves for each individual compound and each sample's corresponding biological mass.

Network analysis

The gene co-expression network was constructed by identifying genes in the dataset that co-expressed with core hypoxia genes of maize. The co-expression matrix was obtained from the CoExpNetViz platform (Tzfadia et al., 2016) and visualized in Cytoscape (Shannon et al., 2003). Pearson correlation coefficients were estimated using the 5 lowest and 95 uppermost percentile ranks as thresholds for co-expression. Topological features of the networks, including clustering coefficients, centrality, and average number of neighbors, were determined using the NetworkAnalyzer plug-in of Cytoscape (v.3.6.0).

Expression data for DEGs in hypoxic roots incubated with either limited or abundant glucose were used to obtain differential co-expression networks for each glucose level at each time point. Clusters of highly interconnected genes within each network were identified by the MCODE plug-in of Cytoscape (v.3.6.0). Enrichment analysis of each module was performed through the Pageman platform (Usadel et al., 2006) or the AgriGO database (Zhou et al., 2010; Tian et al., 2017). Regulatory *cis*-elements were identified from the PlantPAN 2.0 database (Chow et al., 2015).

Accession numbers

Accession numbers of genes for ANPs can be found in Supplemental Table S1. All others can be found in Supplemental Datasets S1–S4.

Supplemental data

The following materials are available in the online version of this article.

Supplemental Figure S1 Responsiveness of the excised maize root-tip system.

Supplemental Figure S2 PCA of root tip samples.

Supplemental Figure S3 Validation of RNA-se read counts by RT-qPCR of genes for core ANPs and *Sps2* (Sucrose P-synthase)

Supplemental Figure S4 GO terms over-represented among hypoxia-responsive genes carrying G4 quadruplex motifs.

Supplemental Figure S5 Profiles of intermediate metabolites in primary metabolism over time.

Supplemental Figure S6 Modules of highly interconnected co-expression networks for genes expressed under low oxygen with either abundant or LG levels.

Supplemental Table S1 Subset of maize genes coding for core ANPs used as baits for the construction of a low-oxygen co-expression network (Figure 7).

Supplemental Table S2 GO terms significantly represented in the *Gpc4–Pdc3* modules in LG and physiologically AG

Supplemental Table S3 List of primers used in this study.

Supplemental Dataset S1 Sugar-responsive genes (mRNAs for DEG) identified by comparing transcriptomes from LG to physiologically abundant glucose (AG) treatments under either ambient air or low oxygen (LO_2).

Supplemental Dataset S2 Oxygen-responsive genes (mRNAs for DEG) identified by comparing transcriptomes from ambient air to low oxygen (LO_2) in the presence of either LG or physiologically AG.

Supplemental Dataset S3 Low oxygen-responsive genes (mRNAs for DEG) in either LG or physiologically AG that contain G4 motifs.

Supplemental Dataset S4 List of component genes that co-expressed with *Pdc3* and *Gpc4* modules under low oxygen conditions in either LG or physiologically AG.

Acknowledgments

We want to thank Dr Eduardo Vallejos for insights and comments during RNA-seq analysis.

Funding

This work was supported by the National Science Foundation (NSF) Plant Genome Research Program (PGRP) projects (NSF-IOS-PGRP-10025976, NSF-IOS-PGRP-1116561, and NSF-IOS-PGRP-178105)

Conflict of interest statement. The authors declare that there are no conflict of interest.

References

Afgan E, Baker D, Batut B, van den Beek M, Bouvier D, Čech M, Chilton J, Clements D, Coraor N, Grüning BA, Guerler A, Hillman-Jackson J, Hiltemann S, Jalili V, Rasche H, Soranzo N,

Goecks J, Taylor J, Nekrutenko A, Blankenberg D (2018) The Galaxy platform for accessible, reproducible and collaborative biomedical analyses: 2018 update. Nucleic Acids Res **46**: W537–W544

Anders S, Pyl PT, Huber W (2015) HTSeq-a Phyton framework to work with high-throughput sequencing data. Bioinformatics **31**: 166–169

Andorf CM, Kopylov M, Dobbs D, Koch KE, Stroupe ME, Lawrence CJ, Bass HW (2014) G-Quadruplex (G4) motifs in the maize (*Zea mays* L.) genome are enriched at specific locations in thousands of genes coupled to energy status, hypoxia, low sugar, and nutrient depravation. J Genet Genomics **41**: 627–647

Antonio C, Päpke C, Rocha M, Diab H, Limami AM, Obata T, Fernie AR, van Dongen JT (2016) Regulation of primary metabolism in response to low oxygen availability as revealed by carbon and nitrogen isotope redistribution. Plant Physiol **170**: 43–56

Alonso AP, Val DL, Shachar-Hill Y (2011) Central metabolic fluxes in the endosperm of developing maize seeds and their implications for metabolic engineering. Metab Eng **13**: 96–107

Alonso AP, Raymond P, Rolin D, Dieuaide-Noubhani M (2007) Substrate cycles in the central metabolism of maize root tips under hypoxia. Phytochemistry **68**: 2222–2231

Alonso AP, Vigeolas H, Raymond P, Rolin D, Dieuaide-Noubhani M (2005) A new substrate cycle in plants. Evidence for a high glucose-phosphate-to-glucose turnover from in vivo steady-state and pulse-labeling experiments with [13C]glucose and [14C]glucose. Plant Physiol **138**: 2220–2232

Armstrong J, Armstrong W (1994) Chlorophyll development in mature lysigenous and schizogenous root aerenchymas provides evidence of continuing cortical cell viability. New Phytol **126**: 493–497

Arrivault S, Guenther M, Ivakov A, Feil R, Vosloh D, van Dongen JT, Sulpice R, Stitt M (2009) Use of reverse-phase liquid chromatography, linked to tandem mass spectrometry, to profile the Calvin cycle and other metabolic intermediates in Arabidopsis rosettes at different carbon dioxide concentrations. Plant J **59**: 826–839

Baena-González E, Rolland F, Thevelein JM, Sheen J (2007) A central integrator or transcription networks in plant stress and energy signaling. Nature **448**: 938–942

Bailey-Serres J, Voesenek LA (2008) Flooding stress: acclimations and genetic diversity. Ann Rev Plant Biol **59**: 313–339

Beaudoin J-D, Perreault J-P (2013) Exploring mRNA 3′-UTR G-quadruplexes: evidence of roles in both alternative polyadenylation and mRNA shortening. Nucleic Acids Res **41**: 5898–5911

Benjamini Y, Hochberg Y (1995) Controlling false discovery rate: a practical and powerful approach to multiple testing. J R Statist Soc Ser B Methodological **57**: 289–300

Bieniawska Z, Paul Barratt DH, Garlick AP, Thole V, Kruger NJ, Martin C, Zrenner R, Smith AM (2007) Analysis of the sucrose synthase gene family in Arabidopsis. Plant J **49**: 810–828

Bouny JM, Saglio PH (1996) Glycolytic flux and hexokinase activities in anoxic maize root tips acclimated by hypoxic pretreatment. Plant Physiol **111**: 187–194

Branco-Price C, Kaiser KA, Jang CJ, Larive CK, Bailey-Serres J (2008) Selective mRNA translation coordinates energetic and metabolic adjustments to cellular oxygen deprivation and reoxygenation in *Arabidopsis thaliana*. Plant J **56**: 743–755

Bret-Harte MS, Silk WK (1994) Nonvascular, symplastic diffusion of sucrose cannot satisfy the carbon demands of growth in the primary root tip of *Zea mays* L. Plant Physiol **105**: 19–33

Brouquisse R, James F, Raymond P, Pradet A (1991) Study of glucose starvation in excised maize root tips. Plant Physiol **96**: 619–626

Campbell MT, Proctor CA, Dou Y, Schmitz AJ, Phansak P, Kruger GR, Zhang C, Walia H (2015) Genetic and molecular characterization of submergence response identifies Subtol6 as a major submergence tolerance locus in maize. PLoS One **10**: e0120385

Chan M-T, Yu S-M (1998) The 3′ untranslated region of a rice α-amylase gene functions as a sugar-dependent mRNA stability determinant. Proc Natl Acad Sci USA **95**: 6543–6547

Cho H, Cho HS, Nam H, Jo H, Yoon J, Park C, Dang TVT, Kim E, Jeong J, Park S, et al. (2018) Translational control of phloem development by RNA G-quadruplex–JULGI determines plant sink strength. Nature Plants **4**: 376–390

Cho H-Y, Lu M-YJ, Shih M-C (2019) The SnRK1-eIFiso4G1 signaling relay regulates the translation of specific mRNAs in Arabidopsis under submergence. New Phytol **222**: 366–381

Cho H-Y, Loreti E, Shih M-C, Perata P (2021) Energy and sugar signaling during hypoxia. New Phytol 229: 57–63

Chow C, Zheng H, Wu N, Chien C, Huang H, Lee T, Chiang-Hsieh Y, Hou P, Yang T, Chang W (2015) PlantPAN2.0: an update of plant promoter analysis navigator for reconstructing transcriptional regulatory networks in plants. Nucleic Acids Res **44**: D1154–D1160

Čikoš Š, Bukovská A, Koppel J (2007) Relative quantification of mRNA: comparison of methods currently used for real-time PCR data analysis. BMC Mol Biol **8**: 113

Claeyssen E, Rivoal J (2007) Isozymes of plant hexokinases: occurrence, properties and functions. Phytochemistry **68**: 709–731

Clark DW, Phang T, Edwards MG, Geraci MW, Gillespie MN (2012) Promoter G-quadruplex sequences are targets for base oxidation and strand cleavage during hypoxia-induced transcription. Free Radic Biol Med **53**: 51–59

Colebrook EH, Thomas SG, Phillips AL, Hedden P (2014) The role of gibberellin signalling in plant responses to abiotic stress. J Exp Biol **217**: 67–75

Couée I, Sulmon C, Gouesbet G, El Mamrani A (2006) Involvement of soluble sugars in reactive oxygen species balance and responses to oxidative stress in plants. J Exp Bot **57**: 449–459

de Sousa SM, Paniago Mdel G, Arruda P, Yunes JA (2008) Sugar levels modulate sorbitol dehydrogenase expression in maize. Plant Mol Biol **68**: 203–213

Dieuaide-Noubhani M, Raffard G, Canioni P, Pradet A, Raymond P (1995) Quantification of compartmented metabolic fluxes in maize root tips using isotope distribution from ^{13}C- or ^{14}C-labeled glucose. J Biol Chem **270**: 13147–13159

Dinneny JR, Long TA, Wang JY, Jung JW, Mace D, Pointer S, Barron C, Brady SM, Schiefelbein J, Benfey PN (2008) Cell identity mediates the response of Arabidopsis roots to abiotic stress. Science **320**: 942–945

Dordas C, Rivoal J, Hill RD (2003) Plant haemoglobins, nitric oxide and hypoxic stress. Ann Bot **91**: 173–178

Drew MC (1997) Oxygen deficiency and root metabolism: injury and acclimation under hypoxia and anoxia. Ann Rev Plant Biol **48**: 223–250

Fedeles BI (2017) G-quadruplex–forming promoter sequences enable transcriptional activation in response to oxidative stress. Proc Natl Acad Sci USA **114**: 2788–2790

Fleming AM, Ding Y, Burrows CJ (2017) Oxidative DNA damage is epigenetic by regulating gene transcription via base excision repair. Proc Natl Acad Sci USA **114**: 2604–2609

Fleming AM, Zhou J, Wallace SS, Burrows CJ (2015) A Role for the fifth G-track in G-quadruplex forming oncogene promoter sequences during oxidative stress: do these "spare tires" have an evolved function? ACS Cent Sci **1**: 226–233

Fukao T, Bailey-Serres J (2008) Submergence tolerance conferred by Sub1A is mediated by SLR1 and SLRL1 restriction of gibberellin responses in rice. Proc Natl Acad Sci USA **105**: 16814–16819

Gamm M, Peviani A, Honsel A, Snel B, Smeekens S, Hanson J (2014) Increased sucrose levels mediate selective mRNA translation in Arabidopsis. BMC Plant Biol **14**: 36

Gharbi I, Ricard B, Rolin D, Maucort M, Andrieu MH, Bizid E, Smiti S, Brouquisse R (2007) Effect of hexokinase activity on tomato root metabolism during prolonged hypoxia. Plant Cell Environ **30**: 508–517

Gasch P, Fundinger M, Müller JT, Lee T, Bailey-Serres J, Mustroph A (2016) Redundant ERF-VII transcription factors bind to an evolutionarily conserved *cis*-motif to regulate hypoxia-responsive gene expression in Arabidopsis. Plant Cell **28**: 160–180

Gayral M, Emorjani K, dalgalarrondo M, Balzergue SM, Pateyron S, Morel MH, Brunet S, Linossier L, Delluc C, Bakan B, et al. (2017) Responses to hypoxia and endoplasmic reticulum stress discriminate the development of vitreous and floury endosperms of conventional maize (*Zea mays*) inbred lines. Front Plant Sci **8**: 557

Geffers R, sell S, Cerff R, Hehl R (2001) The TATA box and a Myb binding site are essential for anaerobic expression of a maize GapC4 minimal promoter in tobacco. Biochim Biophys Acta **1521**: 120–125

Germain V, Ricard B, Raymond P, Saglio PH (1997) The role of sugars, hexokinase, and sucrose synthase in the determination of hypoxically induced tolerance to anoxia in tomato roots. Plant Physiol **114**: 167–175

Guiaquinta RT, Lin W, Sadler NL, Franceschi VR (1983) Pathway of phloem unloading unloading of sucrose in corn roots. Plant Physiol **72**: 362–367

Gibbs DJ, Isa NM, Movahedi M, Lozano-Juste J, Mendiondo GM, Berckhan S, de la Rosa NM, Conde JV, Correia CS, Pearce SP, et al. (2014) Nitric oxide sensing in plants is mediated by proteolytic control of group VII ERF transcription factors. Mol Cell **53**: 369–379

Gibbs DJ, Lee SC, Isa NM, Gramuglia S, Fukao T, Bassel GW, Correia CS, Corbineau F, Theodoulou FL, Bailey-Serres J, Holdsworth MJ (2011) Homeostatic responses to hypoxia is regulated by the N-end rule pathway in plants. Nature **479**: 415–418

Gómez-Pinto I, Vengut-Climent E, Lucas R, Aviñó A, Eritja R, González C, Morales JC (2013) Carbohydrate-DNA interactions at G-quadruplexes: folding and stability changes by attaching sugars at the 5′-end. Chemistry **19**: 1920–1927

Griffin BD, Bass HW (2018) Review: plant G-quadruplex (G4) motifs in DNA and RNA; abundant, intriguing sequences of unknown function. Plant Science **269**: 143–147

Hill SA, ap Rees T (1995) The effect of hypoxia on the control of carbohydrate metabolism in ripening bananas. Planta **197**: 313–323

Horvath S, Dong J (2008) Geometric interpretation of gene co-expression network analysis. PLoS Comput Biol **4**: e1000117

Huber SC, Akazawa T (1986) A novel sucrose synthase pathway for sucrose degradation in cultured sycamore cells. Plant Physiol **81**: 1008–1013

Igamberdiev AU, Hill RD (2004) Nitrate, NO and haemoglobin in plant adaptation to hypoxia: an alternative to classic fermentation pathways. J Exp Bot **55**: 2473–2482

Ismond KP, Dolferus R, De Pauw M, Dennis ES, Good AG (2003) Enhanced ow oxygen survival in arabidopsis through increased metabolic flux in the fermentative pathway. Plant Physiol **132**: 1292–1302

Juntawong P, Girke T, Bazin J, Bailey-Serres J (2014) Translational dynamics revealed by genome-wide profiling of ribosome footprints in *Arabidopsis*. Proc Natl Acad Sci **111**: E203–E212

Kang J, Yu H, Tian C, Zhou W, Li C, Jiao Y, Liu D (2014) Suppression of photosynthetic gene expression in roots is required for sustained root growth under phosphate deficiency. Plant Physiol **165**: 1156–1170

Kendrick S, Hurley LH (2010) The role of G-quadruplex/i-motif secondary structures as cis-acting regulatory elements. Pure Appl Chem **82**: 1609–1621

Keunen E, Peshev D, Vangronsveld J, Ende WVD, Cuypers A (2013) Plant sugars are crucial players in the oxidative challenge during abiotic stress: extending the traditional concept. Plant Cell Environ **36**: 1242–1255

Khan MA, Hamayun M, Iqbal A, Khan SA, Hussain A, Asaf S, Khan AL, Yun BW, Lee I-J (2018) Gibberellin application ameliorates the adverse impact of short-term flooding on Glycine max L. Biochem J **475**: 2893–2905

Kim M, Lim J-H, Ahn CS, Park K, Kim GT, Kim WT, Pai H-S (2006) Mitochondria-associated hexokinases play a role in the control of programmed cell death in *Nicotiana benthamiana*. Plant Cell **18**: 2341–2355

Kim D, Pertea G, Trapnell C, Pimentel H, Kelley R, Salzberg SL (2013) TopHat2: accurate alignment of transcriptomes in the presence of insertions, deletions and gene fusions. Genome Biol **14**: R36

Koch K (2004) Sucrose metabolism: regulatory mechanisms and pivotal roles in sugar sensing and plant development. Curr Opin Plant Biol **7**: 235–246

Koch KE (1996) Carbohydrate-modulated gene expression in plants. Annu Rev Plant Biol **47**: 509–540

Koch KE, Nolte KD, Duke ER, McCarty DR, Avigne WT (1992) Sugar levels modulate differential expression of maize sucrose synthase genes. Plant Cell **4**: 59–69

Koch KE, Ying Z, Wu Y, Avigne WT (2000) Multiple paths of sugar--sensing and a sugar/oxygen overlap for genes of sucrose and ethanol metabolism. J Exp Bot **51**: 417–427

Lasanthi-Kudahettige R, Magneschi L, Loreti E, Gonzali S, Licausi F, Novi G, Beretta O, Vitulli F, Alpi A, Perata P (2009) Transcript profiling of the anoxic rice coleoptiles. Plant Physiol **144**: 218–231

Lee SC, Mustroph A, Sasidharan R, Vashisht D, Pedersen O, Teruko O, Voesenek LACJ, Bailey-Serres J (2011) Molecular characterization of the submergence response of the Arabidopsis thaliana ecotype Columbia. New Phytol **190**: 457–471

Lee KW, Chen PW, Lu CA, Chen S, Ho THD, Yu SM (2009) Coordinated responses to oxygen and sugar deficiency allow rice seedlings to tolerate flooding. Sci Signal **2**: ra61

Lee TA, Bailey-Serres J (2019) Integrative analysis from the epigenome to translatome uncovers patterns of dominant nuclear regulation during transient stress. The Plant Cell **31**: 2573–2595

Licausi F, Kosmacz M, Weits DA, Giuntoli B, Giorgi FM, Voesenek LA, Perata P, van Dongen JT (2011) Oxygen sensing in plants is mediated by an N-end rule pathway for protein destabilization. Nature **479**: 419–422

Lin Y, Zhang C, Lan H, Gao S, Liu H, Liu J, Cao M, Pan G, Rong T, Zhang S (2014) Validation of potential reference genes for qPCR in maize across abiotic stresses, hormone treatments, and tissue types. PLoS One **9**: e95445

Lisec J, Schauer N, Kopka J, Lothar W, Fernie A (2006) Gas chromatography mass spectrometry–based metabolite profiling in plants. Nat Protoc **1**: 387–396

Locke AM, Barding GA, Sathnur S, Larive CK, Bailey-Serres J (2018) Rice SUB1A constrains remodelling of the transcriptome and metabolome during submergence to facilitate post-submergence recovery. Plant Cell Environ **41**: 721–736

Loreti E, Valeri MC, Novi G, Perata P (2018) Gene regulation and survival under hypoxia requires starch availability and metabolism. Plant Physiol **176**: 1286–1298

Loreti E, Poggi A, Novi G, Alpi A, Perata P (2005) A genome-wide analysis of the effects of sucrose on gene expression in Arabidopsis seedlings under anoxia. Plant Physiol **137**: 1130–1138

Love MI, Huber W, Anders S (2014) Moderated estimation of fold change and dispersion for RNA-seq data with DESeq2. Genome Biol **15**: 550

Ma FF, Jazmin LJ, Young JD, Allen DK (2014) Isotopically nonstationary ^{13}C flux analysis of changes in *Arabidopsis thaliana* leaf metabolism due to high light acclimation. Proc Natl Acad Sci USA **111**: 16967–16972

Morgan JT, Fink GR, Bartel DP (2019) Excised linear introns regulate growth in yeast. Nature **565**: 606–611

Mustroph A, Barding GA, Kaiser KA, Larive CK, Bailey-Serres J (2014) Characterization of distinct root and shoot responses to

low-oxygen stress in Arabidopsis with a focus on primary C- and N- metabolism. Plant Cell Environ **37**: 2366–2380

Mustroph A, Zanetti ME, Jang CJ, Holtan HE, Repetti PP, Galbraith DW, Girke T, Bailey-Serres J (2009) Profiling translatomes of discrete cell populations resolves altered cellular priorities during hypoxia in Arabidopsis. Proc Natl Acad Sci USA **106**: 18843–18848

Mustroph A, Albrecht G (2003) Tolerance of crop plants to oxygen deficiency stress: fermentative activity and photosynthetic capacity of entire seedlings under hypoxia and anoxia. Physiol Plant **117**: 508–520

Narsai R, Rocha M, Geigenberger P, Whelan J, van Dongen JT (2011) Comparative analysis between plant species of transcriptional and metabolic responses to hypoxia. New Phytol **2**: 472–487

Pal SK, Liput M, Piques M, Ishihara H, Obata T, Martins MCM, Sulpice R, van Dongen JT, Fernie AR, Yadav UP, et al. (2013) Diurnal changes of polysome loading track sucrose content in the rosette of wild-type Arabidopsis and the starchless *pgm* mutant. Plant Physiol **162**: 1246–1265

Parenteau J, Maignon L, Berthoumieux M, Catala M, Gagnon V, Elela SA (2019) Introns are mediators of cell response to starvation. Nature **565**: 612–617

Pfaffl MW (2001) A new mathematical model for relative quantification in real-time RT-PCR. Nucleic Acids Res **29**: 2002–2007

Postel EH, Berberich SJ, Flint SJ, Ferrone CA (1993) Human c-myc transcription factor PuF identified as nm23-H2 nucleoside diphosphate kinase, a candidate suppressor of tumor metastasis. Science **261**: 478–480

Qin F, Sakuma Y, Li J, Liu Q, Shinozaki K, Yamaguchi-Shinozaki K (2004) Cloning and functional analysis of a novel DREB1/CBF transcription factor involved in cold-responsive gene expression in *Zea mays* L. Plant Cell Physiol **45**: 1042–1052

Rahmani F, Hummel M, Schuurmans J, Wiese-Klinkerberg A, Smeekens S, Hanson J (2009) Sucrose control of translation mediated by an upstream open reading frame-encoded peptide. Plant Physiol **150**: 1356–1367

Ramirez-Aguilar SJ, Keuthe M, Rocha M, Fedyaev VV, Kramp K, Gupta KJ, Rasmusson AG, Schulze WX, van Dongen JT (2011) The composition of plant mitochondrial supercomplexes changes with oxygen availability. J Biol Chem **286**: 43045–43053

Ramon M, Dang TVT, Broeckx T, Hulsmans S, Crepin N, Sheen J, Rolland F (2019) Default Activation and Nuclear Translocation of the Plant Cellular Energy Sensor SnRK1 Regulate Metabolic Stress Responses and Development. The Plant Cell **31**: 1614–1632

Reynoso MA, Kajala K, Bajic M, West DA, Pauluzzi G, Yao AI, Hatch K, Zumstein K, Woodhouse M, Rodriguez-Medina J, et al. (2019) Evolutionary flexibility in flooding response circuitry in angiosperms. Science **365**: 1291–1295

Ricard B, Toai TV, Chourey P, Saglio P (1998) Evidence for the critical role of sucrose synthase for anoxic tolerance of maize roots using a double mutant. Plant Physiol **116**: 1323–1331

Rocha M, Licausi F, Araújo WL, Nunes-Nesi A, Sodek L, Fernie AR, van Dongen JT (2010) Glycolysis and the tricarboxylic acid cycle are linked by alanine aminotransferase during hypoxia induced by waterlogging of Lotus japonicus. Plant Physiol **152**: 1501–1513

Rolland F, Baena-Gonzalez E, Sheen J (2006) Sugar sensing and signaling in plants: conserved and novel mechanisms. Ann Rev Plant Biol **57**: 675–709

Sachs MM, Subbaiah CC, Saab IN (1996) Anaerobic gene expression and flooding tolerance in maize. J Exp Bot **47**: 1–15

Sachs M, Freeling M, Okimoto R (1980) The anaerobic proteins of maize. Cell **20**: 761–767

Saglio PH, Pradet A (1980) Soluble sugars, respiration, and energy charge during aging of excised maize root tips. Plant Physiol **66**: 516–519

Saglio PH, Raymond P, Pradet A (1980) Metabolic activity and energy charge of excised maize root tips under anoxia: Control by soluble sugars. Plant Physiol **66**: 1053–1057

Santaniello A, Loreti E, Gonzali S, Novi G, Perata P (2014) A reassessment of the role of sucrose synthase in the hypoxic sucrose-ethanol transition in Arabidopsis. Plant Cell Environ **37**: 2294–2302

Sasidharan R, Mustroph A, Booman A, Akman M, Ammerlaan AMH, Breit T, Schranz ME, Voesenek LACJ, van Tienderen PH (2013) Root transcript profiling of two *Rorippa* species reveals gene clusters associated with extreme submergence tolerance. Plant Physiol **163**: 1277–1292

Shannon P, Markiel A, Ozier O, Baliga NS, Wang JT, Ramage D, Amin N, Schwikowski B, Ideker T (2003) Cytoscape: a software environment for integrated models of biomolecular interaction networks. Genome Biol **13**: 2498–2504

Shannon JC (1972) Movement of ^{14}C-labeled assimilates into kernels of *Zea mays* L. I. Pattern and rate of sugar movement. Plant Physiol **49**: 198–202

Shingaki-Wells R, Millar AH, Whelan J, Narsai R (2014) What happens to plant mitochondria under low oxygen? An omics review of the responses to low oxygen and reoxygenation. Plant Cell Environ **37**: 2260–2277

Shulman RG, Rothman DL (2015) Homeostasis and the glycogen shunt explains aerobic ethanol production in yeast. Proc Natl Acad Sci USA **112**: 10902–10907

Song J, Perreault J-P, Topisirovic I, Richard S (2016) RNA G-quadruplexes and their potential regulatory roles in translation. Translation (Austin) **4**: e1244031

Thomas JD, Dias LM, Johannes GJ (2008) Translational repression during chronic hypoxia is dependent on glucose levels. RNA **14**: 771–781

Thomson CJ, Greenway H (1991) Metabolic evidence for stellar anoxia in maize roots exposed to low O_2 concentrations. Plant Physiol **96**: 1294–1301

Tian T, Liu Y, Yan H, You Q, Yi X, Du Z, Xu W, Su Z (2017) agriGo v2.0: a GO analysis toolkit for the agricultural community, 2017 update. Nucleic Acids Res **45**: W122–W129

Tomé F, Nägele T, Adamo M, Garg A, Marco-Llorca C, Nukarinen E, Pedrotti L, Peviani A, Simeunovic A, Tatkiewicz A, et al. (2014) The low energy signaling network. Front Plant Sci **5**: 353

Tzfadia O, Diels T, De Meyer S, Vandepoele K, Aharoni A, Van de Peer Y (2016) CoExpNetViz: Comparative co-expression networks construction and visualization tool. Front Plant Sci **6**: 1194

Usadel B, Nagel A, Steinhauser D, Gibon Y, Bläsing OE, Redestig H, Screenivasulu N, Krall L, Hannah MA, Poree F, et al. (2006) PageMan: an interactive ontology tool to generate, display, and annotate overview graphs for profiling experiments. BMC Bioinform **7**: 535

van Dongen JT, Licausi F (2015) Oxygen sensing and signaling. Annu Rev Plant Biol **66**: 345–367

van Dongen JT, Fröhlich A, Ramirez-Aguilar SJ, Schauer N, Fernie AR, Erban A, Kopka J, Clark J, Langer A, Geigenberger P (2009) Transcript and metabolite profiling of the adaptive response to mild decreases in oxygen concentration in the roots of arabidopsis plants. Ann Bot **103**: 269–280

van Dongen JT, Gupta KJ, Ramirez-Aguilar SJ, Araujo WL, Nunes-Nesi A, Fernie AR (2011) Regulation of respiration in plants: a role for alternative metabolic pathways. J Plant Physiol **168**: 1434–1443

van Veen H, Vashisht D, Akman M, Girke T, Mustroph A, Reinen E, Hartman S, Kooiker M, van Tienderen P, Schranz ME, et al. (2016) Transcriptome of eight *Arabidopsis thaliana* accessions reveal core conserved, genotype-and organ-specific responses to flooding stress. Plant Physiol **172**: 668–689

Vartapetian BB, Andreeva IN (1986) Mitochondrial ultrastructure of three hygrophyte species at anoxia and in anoxic glucose-supplemented medium. J Exp Bot **37**: 685–692

Wang H, Sui X, Guo J, Wang Z, Cheng J, Ma S, Li X, Zhang Z (2014) Antisense suppression of cucumber (Cucumis sativus L.) sucrose synthase 3 (CsSUS3) reduces hypoxic stress tolerance. Plant, Cell Environ **37**: 795–810

Welsh SJ, Dale AG, Lombardo CM, Valentine H, de la Fuente M, Schatzlein A, Stephen N (2013) Inhibition of the hypoxia-inducible factor pathway by a G-quadruplex binding small molecule. Sci Rep **3**: 2799

Wolfe AL, Singh K, Zhong Y, Drewe P, Rajasekhar VK, Sanghvi VR, Mavrakis KJ, Jiang M, Roderick JE, Van der Meulen J, et al. (2014) RNA G-quadruplexes cause eIF4A-dependent oncogene translation in cancer. Nature **513**: 65–70

Xiong Y, McCormack M, Li L, Hall Q, Xiang C, Sheen J (2013) Glucose-TOR signaling reprograms the transcriptome and activates meristems. Nature **496**: 181–186

Yukawa Y, Sugita M, Choisne N, Small I, Sugiura M (2000) The TATA motif, the CAA motif and the poly(T) transcription termination motifs are all important for transcription re-initiation on plant tRNA genes. Plant J **22**: 439–447

Zeng Y, Wu Y, Avigne WT, Koch KK (1999) Rapid repression of maize Invertases by low oxygen. Invertase/Sucrose Synthase balance, sugar signaling potential, and seedling survival. Plant Physiol **121**: 599–608

Zeng Y, Wu Y, Avigne WT, Koch KE (1998) Differential regulation of sugar-sensitive sucrose synthases by hypoxia and anoxia indicate complementary transcriptional and posttranscriptional responses. Plant Physiol **116**: 1573–1583

Zhou D, Zhou X, Ling Y, Zhang Z, Su Z (2010) agriGO: a GO analysis toolkit for the agricultural community. Nucl Acids Res **38**: W64–W70